

Supporting Information for

Unraveling the structure and chemical mechanisms of highly oxygenated intermediates in oxidation of organic compounds

Zhandong Wang^{a,*}, Denisia M. Popolan-Vaida^{b,c,d,e}, Bingjie Chen^a, Kai Moshammer^{f,g}, Samah Y. Mohamed^a, Heng Wang^a, Salim Sioud^h, Misjudeen A. Raji^h, Katharina Kohse-Höinghausⁱ, Nils Hansen^f, Philippe Dagaut^j, Stephen R. Leone^{b,c,d}, S. Mani Sarathy^{a,*}

^aKing Abdullah University of Science and Technology (KAUST), Clean Combustion Research Center (CCRC), Thuwal 23955-6900, Saudi Arabia

^bDepartment of Chemistry, University of California, Berkeley, CA 94720, USA

^cDepartment of Physics, University of California, Berkeley, CA 94720, USA

^dChemical Sciences Division, Lawrence Berkeley National Laboratory, Berkeley, CA 94720, USA

^eDepartment of Chemistry, University of Central Florida, Orlando, FL 32816-2450, USA

^fCombustion Research Facility, Sandia National Laboratories, Livermore, CA 94551, USA

^gPhysikalisch-Technische Bundesanstalt, Bundesallee 100, 38116 Braunschweig, Germany

^hKing Abdullah University of Science and Technology (KAUST), Analytical Core Lab (ACL), Thuwal 23955-6900, Saudi Arabia

ⁱDepartment of Chemistry, Bielefeld University, D-33615 Bielefeld, Germany

^jCentre National de la Recherche Scientifique (CNRS), Institut National des Sciences de l'Ingénierie et des Systèmes (INSIS), Institut de Combustion, Aérothermique, Réactivité et Environnement (ICARE), 1C ave recherche scientifique, 45071, Orléans, cedex 2, France

S1: Experimental

S1.1: Details of experimental method

The majority of measurements were obtained using SVUV-PI-MBMS, which freezes the reaction upon molecular beam sampling and enables the detection of reactive intermediates (e.g., peroxides) (1, 2). The diagram of the JSR-1 experimental setup is presented in Fig. S1A. The mass spectrometer has a sensitivity range of 1 ppm, a mass resolving power of ~3500, and a dynamic range of six orders of magnitude. The photoionization spectra at 9.5 or 9.6 eV were measured at varying reactor temperatures to obtain the distribution of auto-oxidation products.

The photoionization efficiency spectra (PIE) of the auto-oxidation products and their fragments were measured from 8.5 to 10.5 eV.

SVUV-PI-MBMS experiments were performed at Terminal 3 of the Chemical Dynamics Beamline of the Advanced Light Source at the Lawrence Berkeley National Laboratory. The photon beam has a high flux (10^{14} photons/s) and very good energy resolution [$E/\Delta E(\text{fwhm}) \sim 250\text{--}400$] in the chemically interesting region from 7.4 to 30 eV. It is an important assumption that only singly charged ions are formed. The JSR, with a volume of about 33.5 cm^3 , was composed of quartz; a K-type thermocouple, coated with Inconel alloy 600 (Thermocoax), was fixed at the vicinity of the sampling cone to measure the reactor temperature. Experiments conducted without the thermocouple in place detected similar species' distributions in the reactor, indicating that the thermocouple did not catalyze the oxidation reaction under the conditions studied here. Uncertainty in the reactor temperature was $\pm 20 \text{ K}$, obtained by measuring the temperature distribution inside the JSR with a movable thermocouple. Gas streams of fuels and oxygen (diluted with argon) were guided through two concentric tubes, mixing at their outlets. The mixed gases then entered the reactor through four injectors, with exit nozzles located in the center of the JSR. The four nozzles, each with an inner diameter of about 1 mm, created gas jets at their outlets and induced turbulent mixing. The fuel flow rate was measured by a syringe pump, mixed with Ar flow, controlled by calibrating (against N_2) mass flow controllers (MKS), and vaporized in a simple vaporizer at a temperature $\sim 30 \text{ K}$ higher than the fuel's boiling point. The gas flows of O_2 and the remaining Ar were also regulated by calibrating (against N_2) mass flow controllers (MKS). The reactor was completely enclosed by an oven that allowed for adjusting temperature over the desired range. The oven and the reactor were surrounded by a water-cooled stainless steel chamber. Exhaust gases were continuously removed to maintain pressure constant at 700 Torr. The reaction gases were from the reactor and guided into the molecular-beam mass spectrometer through a quartz nozzle with a 40° cone angle and a $\sim 50 \mu\text{m}$ orifice diameter at the tip.

Details of the MBMS section of the instrument are described elsewhere (1). The apparatus consisted of a two-stage differentially-pumped vacuum chamber that hosted the ion source of the mass spectrometer. A reduction from near atmospheric pressure in the reactor to $\sim 10^{-3} \text{ mbar}$ in the first pumping stage led to the formation of a molecular beam and precluded further reactions.

The beam then passed through a skimmer into the ionization region of the mass spectrometer, held at 10^{-6} mbar.

For the APCI-OTMS experiment, the mass scan range was set to cover the m/z range 50–300 and the analytes were detected in the Orbitrap at a mass resolving power of 100000, a sensitivity range of 1-5 ppm, and mass accuracy < 5 ppm. The diagram of JSR-2 combined with APCI-OTMS is presented in Fig. S1B (3). APCI-OTMS experiments were performed at the Analytical Core Lab of King Abdullah University of Science & Technology (KAUST). The volume of the jet-stirred reactor was about 76 cm³. Similar to the JSR for the SVUV-PI-MBMS experiment, gas streams of fuels and oxygen (diluted with argon) were guided through two concentric tubes, mixing at their outlets. The mixed gases then entered the reactor through four injectors, with exit nozzles located in the center of the JSR. The four nozzles, each with an inner diameter of about 0.3 mm, created gas jets at their outlets and induced turbulent mixing. The reactor was covered by an oven, and temperatures of the oven and the reactor were measured by a K-type thermocouple. The pressure of the reactor was maintained at atmospheric pressure. The flow rate of the fuel was measured by a syringe pump and mixed with Ar in a simple vaporizer at a temperature ~ 30 K higher than the boiling point of the fuel. The flow of Ar and O₂ was controlled by calibrating (against N₂) mass flow controllers (MKS). The JSR and the sampling method was similar to that used by Dagaut *et al.* (4). The products were sampled using a quartz tube at the outlet of the reactor and ionized by the APCI; the ions were then sucked into the system using a skimmer with a positive mode for analysis. In the analysis, the Orbitrap automated gain control (AGC) target was set to 1×10^6 charges for full scan and the micro scan was set to 500 ms. The vaporizer temperature of the APCI source was 430 K, the sheath gas flow rate was 50 (arb. unit), the Aux gas flow rate was 20 (arb. unit), and the sweep gas flow rate was 10 (arb. unit). The temperature of the capillary was 548 K. The signal of the intermediate was recorded for a minute and an average signal was obtained from the scans. The calibration of the LTQ-Orbitrap mass analyzer was performed in positive ESI ionization mode, according to manufacturer's guidelines. The Orbitrap mass spectrometer was operated using XCalibur software.

Tunable synchrotron vacuum ultraviolet light was used in a single photon ionization technique. A neutral species was ionized when the photon energy was higher than its ionization energy, resulting in a molecular peak (M⁺) and/or its fragments. The APCI is a soft ionization

method with low fragmentation risk, mainly used with polar and relatively nonpolar compounds, and generally producing mono-charged ions. The analyte was in the gaseous form in this work; its ionization was accomplished using an atmospheric pressure corona discharge (5-7 μ A). APCI spectra provide an easily identifiable protonated molecular ion peak $[M+H]^+$, which allows the determination of the molecular mass (5).

This work investigated the auto-oxidation of ten non-oxygenated organic compounds and five organic compounds with oxygen-containing functional groups. The experimental conditions for the SVUV-PI-MBMS and APCI-OTMS experiments are shown in Table S1. Most of the procedure was performed by the SVUV-PI-MBMS; the auto-oxidation of methylcyclohexane and 4-methylheptane was investigated by APCI-OTMS; while the auto-oxidation of 2,7-dimethyloctane and cyclohexane was studied in both set-ups.

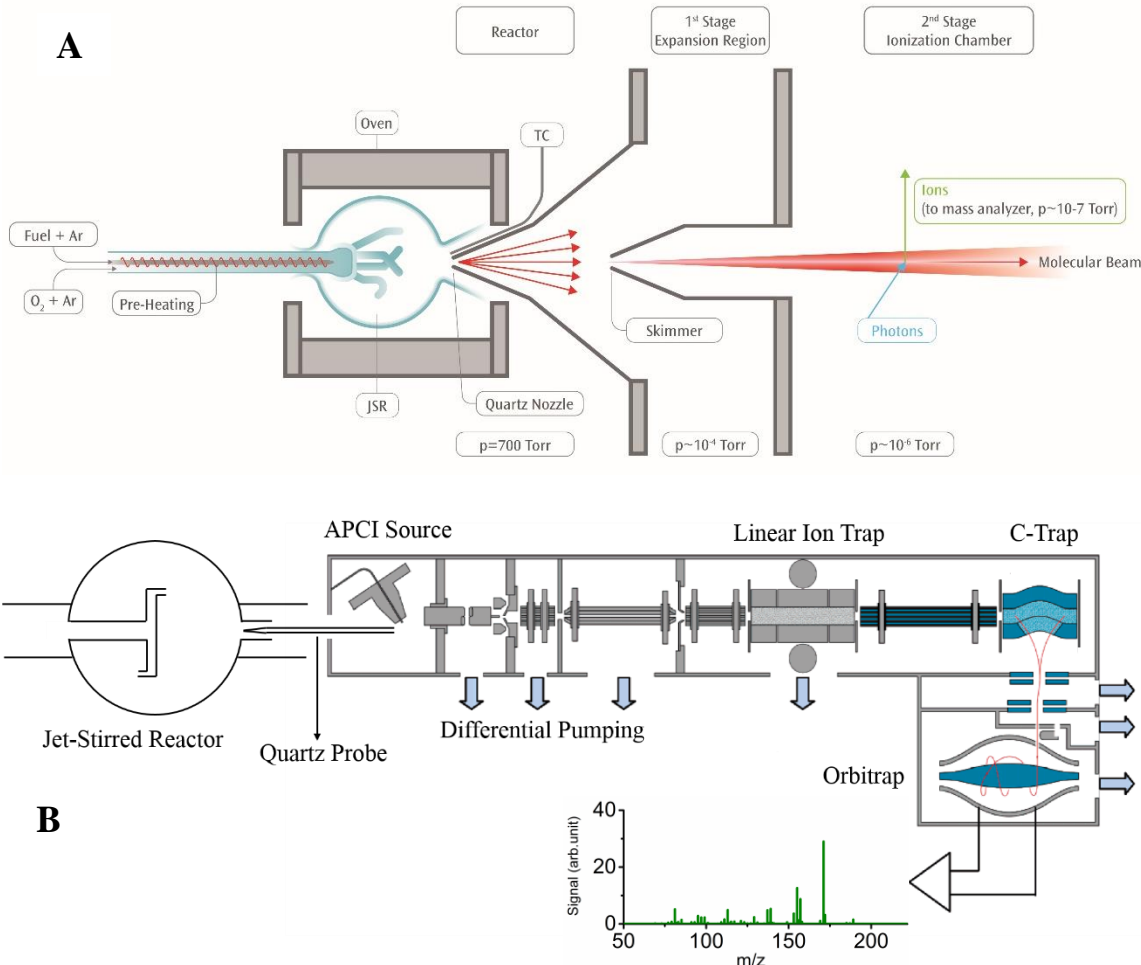


Figure S1: Schematic representation of experimental model for JSR experiment at ALS (A) and KAUST (B). Figure S1A courtesy of ref. 27 [Moshammer, et al.] from the main-text, copyright 2016 American Chemical Society, with permission from Journal of Physical Chemistry. Figure S1B courtesy of ref. 30 [Wang, et al.] from the main-text, copyright 2017, with permission from Elsevier.

Table S1: Experimental conditions for organic compound auto-oxidation and H/D exchange reactions in this work

Diagnostics	Reactant	Composition	ϕ	Residence time (s)	Pressure (Torr)
SVUV-PI-MBMS	<i>n</i> -heptane	1% fuel/11% ¹⁶ O ₂ /88%Ar	1	2	700
	cyclohexane	1% fuel/18% ¹⁶ O ₂ /81%Ar	0.5	2	700
	cyclohexane	1% fuel/9% ¹⁸ O ₂ /90%Ar	1	2	700
	cycloheptane	1.5% fuel/15.75% ¹⁶ O ₂ /82.75%Ar	1	2	700
	<i>n</i> -decane	0.8% fuel/12.4% ¹⁶ O ₂ /86.8%Ar	1	2	700
	<i>n</i> -dodecane	0.6% fuel/11.1% ¹⁶ O ₂ /88.3%Ar	1	2	700
	2-methylnonane	0.8% fuel/12.4% ¹⁶ O ₂ /86.8%Ar	1	2	700
	2,7-dimethyloctane	0.8% fuel/12.4% ¹⁶ O ₂ /86.8%Ar	1	2	700
	2,7-dimethyloctane	0.8% fuel/12.4% ¹⁸ O ₂ /86.8%Ar	1	2	700
	2,7-dimethyloctane/D ₂ O	0.76% fuel/11.8% ¹⁶ O ₂ /82.68%Ar/4.76%D ₂ O	1	1.9	700
	<i>n</i> -butylcyclohexane	0.8% fuel/12% ¹⁶ O ₂ /87.2%Ar	1	2	700
	<i>n</i> -decanol	0.8% fuel/12% ¹⁶ O ₂ /87.2%Ar	1	2	700
	decanal	0.8% fuel/11.6% ¹⁶ O ₂ /87.6%Ar	1	2	700
	2-decanone	0.8% fuel/11.6% ¹⁶ O ₂ /87.6%Ar	1	2	700
APCI-OTMS	dipentyl ether	0.8% fuel/12% ¹⁶ O ₂ /87.2%Ar	1	2	700
	methyl decanoate	0.8% fuel/12.4% ¹⁶ O ₂ /86.8%Ar	1	2	700
	cyclohexane	1% fuel/9% ¹⁶ O ₂ /90%Ar	1	2	760
	methylcyclohexane	1.5% fuel/15.75% ¹⁶ O ₂ /82.75%Ar	1	2	760
SVUV-PI-MBMS	4-methylheptane	1% fuel/12.5% ¹⁶ O ₂ /86.5%Ar	1	2	760
	2,7-dimethyloctane	0.8% fuel/12.4% ¹⁶ O ₂ /86.8%Ar	1	2	760
	2,7-dimethyloctane/D ₂ O	0.76% fuel/94.48%Ar/4.76%D ₂ O		1.9	700
	ethanol/D ₂ O	0.76% fuel/94.48%Ar/4.76%D ₂ O		1.9	700
	acetone/D ₂ O	0.76% fuel/94.48%Ar/4.76%D ₂ O		1.9	700
	propanal/D ₂ O	0.76% fuel/94.48%Ar/4.76%D ₂ O		1.9	700
	acetic acid/D ₂ O	0.76% fuel/94.48%Ar/4.76%D ₂ O		1.9	700
	tetrahydrofuran/D ₂ O	0.76% fuel/94.48%Ar/4.76%D ₂ O		1.9	700

S1.2: Mass spectra of $C_xH_{y-2}O_{z+n}$ ($n=0-5$) and $C_xH_{y-4}O_{z+n}$ ($n=4$) in the 15 VOCs auto-oxidation

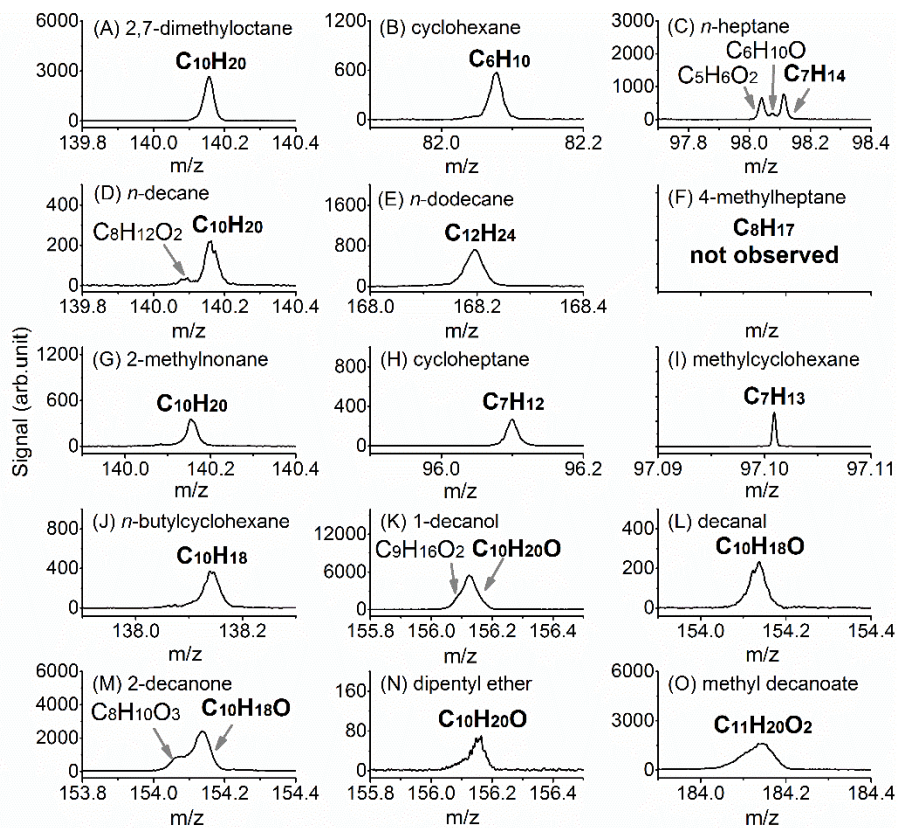


Figure S2: Mass spectrum recorded in oxidation of 15 organic compounds highlighting species with molecular formula of $C_xH_{y-2}O_z$. Data in (F) for 4-methylheptane and (I) for methylcyclohexane obtained from APCI-OTMS experiments, remainder are from SVUV-PI-MBMS experiments. x equals to the carbon number of the organic compounds; y is equal to $2x+2$ for alkanes, alcohols, and ethers, $2x$ for cycloalkanes, aldehydes, ketone compounds, and esters; z is equal to 0 for hydrocarbons, 1 for alcohols, aldehydes, ketone compounds, and ethers, and 2 for esters.

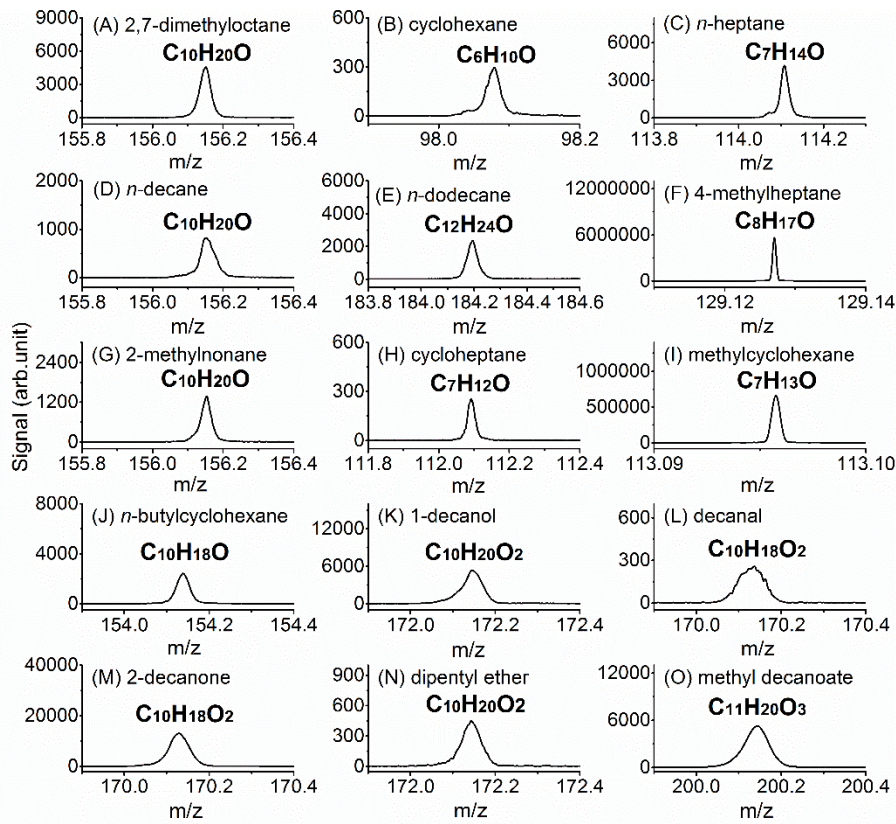


Figure S3: Mass spectrum recorded in oxidation of 15 organic compounds highlighting species with molecular formula of $C_xH_{y-2}O_{z+1}$. Data in (F) for 4-methylheptane and (I) for methylcyclohexane obtained from APCI-OTMS experiments, remainder are from SVUV-PI-MBMS experiments. x equals to the carbon number of the organic compounds; y is equal to $2x+2$ for alkanes, alcohols, and ethers, $2x$ for cycloalkanes, aldehydes, ketone compounds, and esters; z is equal to 0 for hydrocarbons, 1 for alcohols, aldehydes, ketone compounds, and ethers, and 2 for esters.

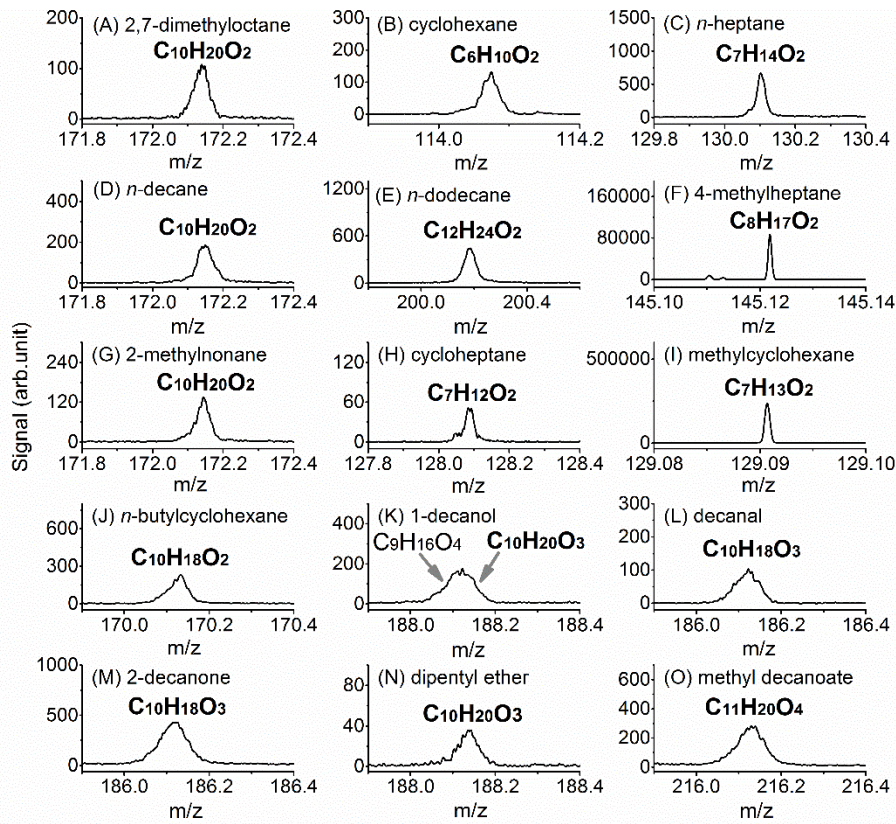


Figure S4: Mass spectrum recorded in oxidation of 15 organic compounds highlighting species with molecular formula of $C_xH_{y-2}O_{z+2}$. Data in (F) for 4-methylheptane and (I) for methylcyclohexane obtained from APCI-OTMS experiments, remainder are from SVUV-PI-MBMS experiments. x equals to the carbon number of the organic compounds; y is equal to $2x+2$ for alkanes, alcohols, and ethers, $2x$ for cycloalkanes, aldehydes, ketone compounds, and esters; z is equal to 0 for hydrocarbons, 1 for alcohols, aldehydes, ketone compounds, and ethers, and 2 for esters.

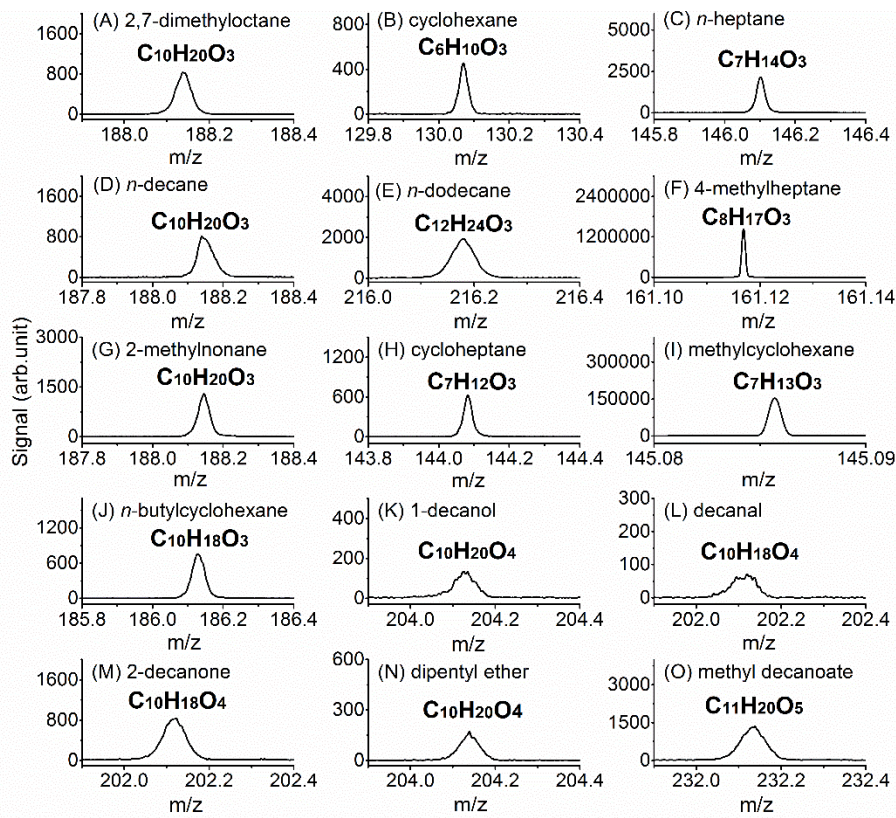


Figure S5: Mass spectrum recorded in oxidation of 15 organic compounds highlighting species with molecular formula of $C_xH_{y-2}O_{z+3}$. Data in (F) for 4-methylheptane and (I) for methylcyclohexane obtained from APCI-OTMS experiments, remainder are from SVUV-PI-MBMS experiments. x equals to the carbon number of the organic compounds; y is equal to $2x+2$ for alkanes, alcohols, and ethers, $2x$ for cycloalkanes, aldehydes, ketone compounds, and esters; z is equal to 0 for hydrocarbons, 1 for alcohols, aldehydes, ketone compounds, and ethers, and 2 for esters.

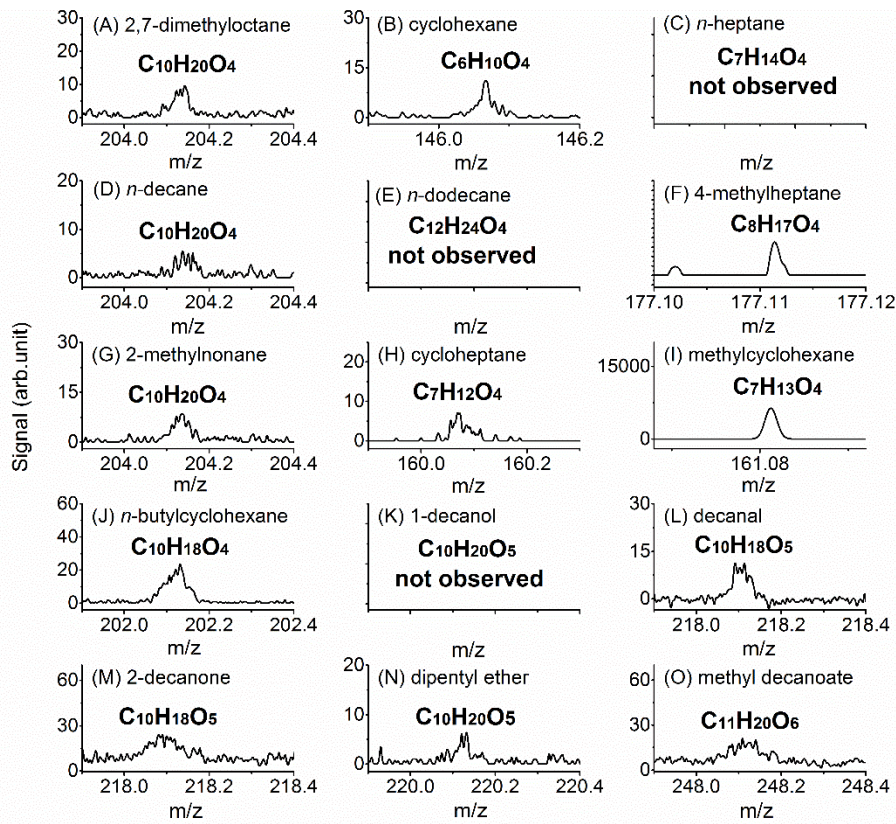


Figure S6: Mass spectrum recorded in oxidation of 15 organic compounds highlighting species with molecular formula of $C_xH_{y-2}O_{z+4}$. Data in (F) for 4-methylheptane and (I) for methylcyclohexane obtained from APCI-OTMS experiments, remainder are from SVUV-PI-MBMS experiments. x equals to the carbon number of the organic compounds; y is equal to $2x+2$ for alkanes, alcohols, and ethers, $2x$ for cycloalkanes, aldehydes, ketone compounds, and esters; z is equal to 0 for hydrocarbons, 1 for alcohols, aldehydes, ketone compounds, and ethers, and 2 for esters.

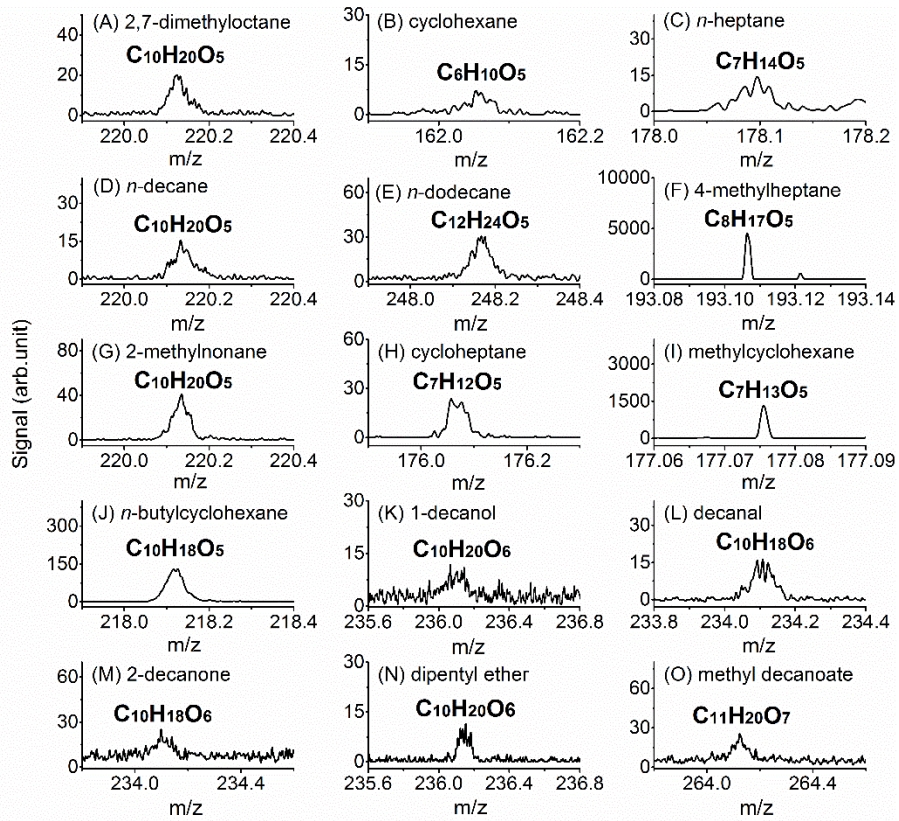


Figure S7: Mass spectrum recorded in oxidation of 15 organic compounds highlighting species with molecular formula of $C_xH_{y-2}O_{z+5}$. Data in (F) for 4-methylheptane and (I) for methylcyclohexane obtained from APCI-OTMS experiments, remainder are from SVUV-PI-MBMS experiments. x equals to the carbon number of the organic compounds; y is equal to $2x+2$ for alkanes, alcohols, and ethers, $2x$ for cycloalkanes, aldehydes, ketone compounds, and esters; z is equal to 0 for hydrocarbons, 1 for alcohols, aldehydes, ketone compounds, and ethers, and 2 for esters.

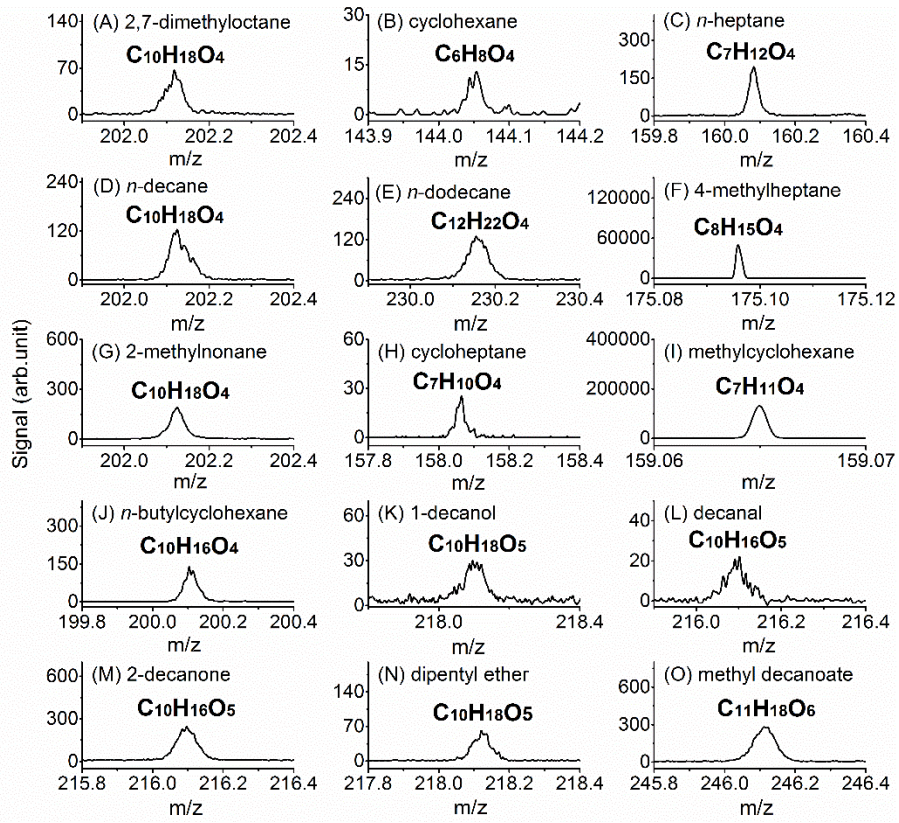
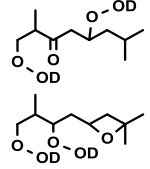
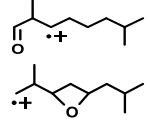
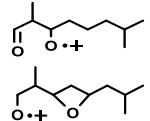
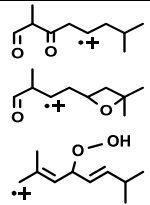
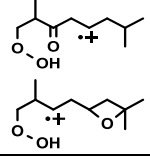
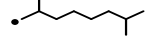
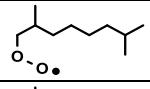
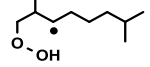
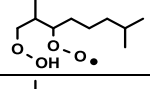
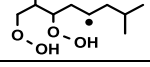
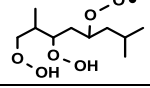
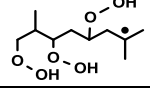


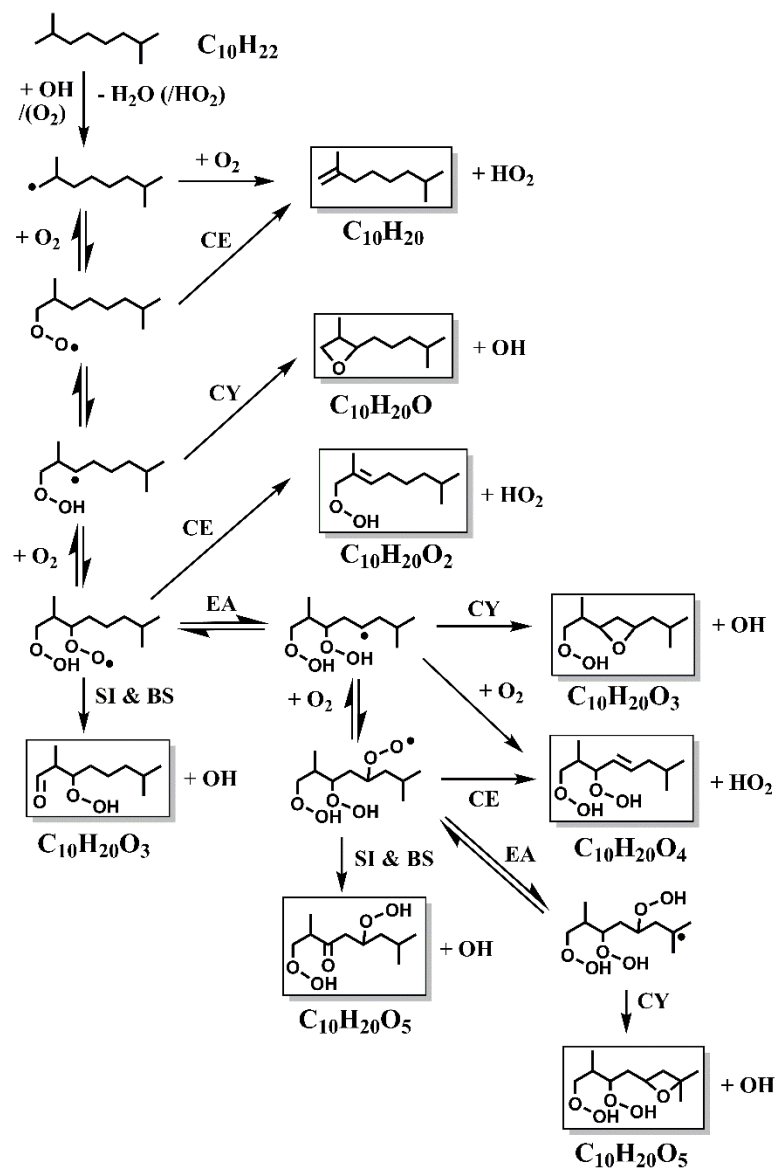
Figure S8: Mass spectrum recorded in oxidation of 15 organic compounds highlighting species with molecular formula of $C_xH_y-4O_{z+4}$. Data in (F) for 4-methylheptane and (I) for methylcyclohexane obtained from APCI-OTMS experiments, remainder are from SVUV-PI-MBMS experiments. x equals to the carbon number of the organic compounds; y is equal to $2x+2$ for alkanes, alcohols, and ethers, $2x$ for cycloalkanes, aldehydes, ketone compounds, and esters; z is equal to 0 for hydrocarbons, 1 for alcohols, aldehydes, ketone compounds, and ethers, and 2 for esters.

S1.3: Glossary of species mentioned in the text

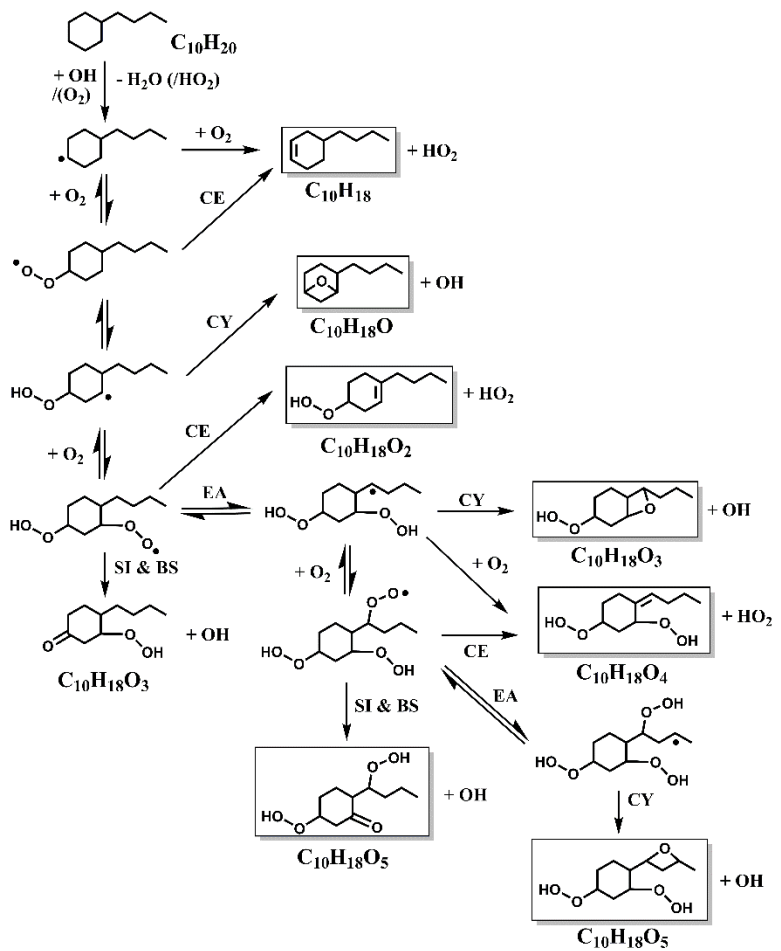
Molecules	Note	Example	Structure
$C_xH_yO_z$	VOC, x, y, z are the carbon, oxygen, and hydrogen number, respectively. The same for the following	$C_{10}H_{22}$	
$C_xH_{y-2}O_{z+0}$	Olefins with the same carbon skeleton of VOC	$C_{10}H_{20}$	
$C_xH_{y-2}O_{z+1}$	Cyclic ethers with the same carbon skeleton of VOC	$C_{10}H_{20}O$	
$C_xH_{y-2}O_{z+2}$	Olefinic hydroperoxides with the same carbon skeleton of VOC	$C_{10}H_{20}O_2$	
$C_xH_{y-2}O_{z+3}$	Keto-hydroperoxides and/or hydroperoxy cyclic ethers with the same carbon skeleton of VOC	$C_{10}H_{20}O_3$	
$C_xH_{y-2}O_{z+4}$	Olefinic dihydroperoxides with the same carbon skeleton of VOC	$C_{10}H_{20}O_4$	
$C_xH_{y-2}O_{z+5}$	Keto-dihydroperoxides and/or dihydroperoxy cyclic ethers with the same carbon skeleton of VOC	$C_{10}H_{20}O_5$	
$C_{x-4}H_{y-4}O_{z+4}$	Diketo-hydroperoxides and/or keto-hydroperoxy cyclic ethers and/or dihydroperoxy dienes with the same carbon skeleton of VOC	$C_{10}H_{18}O_4$	
$C_{10}H_{19}DO_3$	Keto-hydroperoxides and/or hydroperoxy cyclic ethers with the same carbon skeleton of VOC. The H-atom in -OOH functional group was replaced by D atom		
$C_{10}H_{17}DO_4$	Diketo-hydroperoxides and/or keto-hydroperoxy cyclic ethers with the same carbon skeleton of VOC. The H-atom in -OOH functional group was replaced by D atom		
$C_{10}H_{16}D_2O_4$	Dihydroperoxy dienes with the same carbon skeleton of VOC. The H-atoms in -OOHs functional group were replaced by D atoms		
$C_{10}H_{19}DO_5$	Keto-dihydroperoxides and/or dihydroperoxy cyclic ethers with the same carbon skeleton of VOC. The H-atom in one -OOH functional group was replaced by D atom		

$C_{10}H_{18}D_2O_5$	Keto-dihydroperoxides and/or dihydroperoxy cyclic ethers with the same carbon skeleton of VOC. The H-atoms in –OOHs functional group were replaced by D atoms		
$C_{10}H_{19}O^+$	The plausible fragments of the primary ion $C_{10}H_{20}O_3^+$ after elimination of –OOH		
$C_{10}H_{19}O_2^+$	The plausible fragments of the primary ion $C_{10}H_{20}O_3^+$ through dissociation of the O–OH bond in the hydroperoxy group		
$C_{10}H_{17}O_2^+$	The plausible fragments of the primary ion $C_{10}H_{18}O_4^+$ after elimination of –OOH		
$C_{10}H_{19}O_3^+$	The plausible fragments of the primary ion $C_{10}H_{20}O_5^+$ after elimination of –OOH		
$C_xH_{y-1}O_z$	R radical, produced from the H-atom abstraction of VOC molecule $C_xH_yO_z$	$C_{10}H_{21}$	
$C_xH_{y-1}O_{z+2}$	ROO radical--peroxy radical--, produced from the O_2 addition to R radical	$C_{10}H_{21}OO$	
$C_xH_{y-1}O_{z+2}$	QOOH radical--hydroperoxyalkyl radical--, produced from the isomerization of ROO radical	$C_{10}H_{20}OOH$	
$C_xH_{y-1}O_{z+4}$	OOQOOH radical--hydroperoxyalkyl peroxy radical--, produced from the O_2 addition to QOOH radical	$OOC_{10}H_{20}OOH$	
$C_xH_{y-1}O_{z+4}$	P(OOH) ₂ radical--dihydroperoxyalkyl radical--, produced from the isomerization of OOQOOH radical	$HOOC_{10}H_{19}OOH$	
$C_xH_{y-1}O_{z+6}$	OOP(OOH) ₂ radical--dihydroperoxyalkyl peroxy radical--, produced from the O_2 addition to P(OOH) ₂ radical	$OOC_{10}H_{19}(OOH)_2$	
$C_xH_{y-1}O_{z+6}$	T(OOH) ₃ radical--trihydroperoxyalkyl peroxy radical--, produced from the isomerization of OOP(OOH) ₂ radical	$C_{10}H_{18}(OOH)_3$	

S1.4: Specific mechanism diagrams of 2,7-dimethyloctane and *n*-butylcyclohexane



Scheme S1: Auto-oxidation mechanism of 2,7-dimethyloctane, leading to formation of intermediates with molecular formula of C₁₀H₂₀On (n=0-5, labeled in boxed). The structures of probable intermediates for auto-oxidation of 2,7-dimethyloctane radical at the primary carbon are presented. CE: concerted elimination, BS: β -scission, CY: cyclization, SI: standard isomerization, EA: extensive auto-oxidation.



Scheme S2: Auto-oxidation mechanism of *n*-butylcyclohexane, leading to formation of intermediates with molecular formula of C₁₀H₁₈On (n=0-5, labeled in boxed). The structures of probable intermediates for auto-oxidation of *n*-butylcyclohexane radical at a second carbon are presented. CE: concerted elimination, BS: β-scission, CY: cyclization, SI: standard isomerization, EA: extensive auto-oxidation.

S1.5: Mass spectra of highly oxygenated intermediates recorded in cyclohexane auto-oxidation

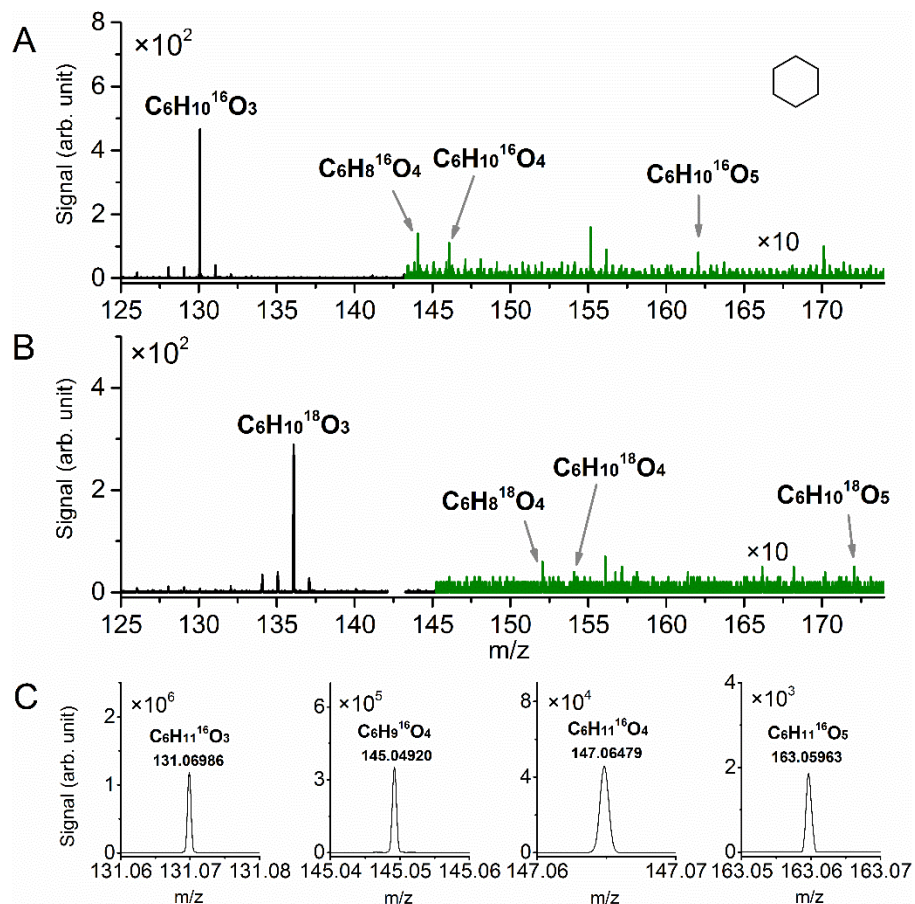


Figure S9: Mass spectra recorded in cyclohexane auto-oxidation. A, SVUV-PI-MBMS results at photon energy of 10.5 eV, $^{16}\text{O}_2$ as the oxidizer, and equivalence ratio is 0.5. B, SVUV-PI-MBMS results at photon energy of 10.5 eV, $^{18}\text{O}_2$ as the oxidizer, and equivalence ratio is 1.0. Mass zone (green in A and B) multiplied by ten for clarity, respectively. C, APCI-OTMS results with $^{16}\text{O}_2$ as oxidizer. The protonated molecular ion peaks of highly oxygenated intermediates with three to five oxygens labeled with molecular formula and exact mass (accuracy < 5 ppm).

S1.6: Temperature profiles of highly oxygenated intermediates and their fragments in 2,7-dimethyloctane oxidation.

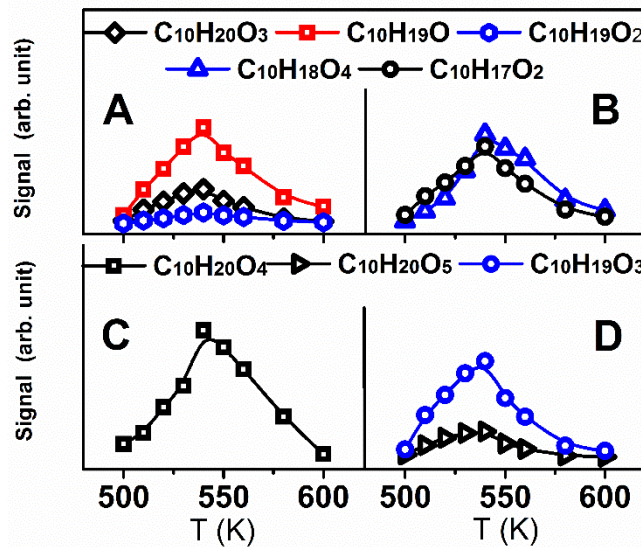


Figure S10 Temperature-dependent signal profiles of $\text{C}_{10}\text{H}_{20}\text{O}_3$ and fragments ($\text{C}_{10}\text{H}_{19}\text{O}^+$ and $\text{C}_{10}\text{H}_{19}\text{O}_2^+$), $\text{C}_{10}\text{H}_{18}\text{O}_4$ and fragment ($\text{C}_{10}\text{H}_{17}\text{O}_2^+$), $\text{C}_{10}\text{H}_{20}\text{O}_4$, $\text{C}_{10}\text{H}_{20}\text{O}_5$ and fragment ($\text{C}_{10}\text{H}_{19}\text{O}_3^+$) measured in SVUV-PI-MBMS experiment of 2,7-dimethyloctane oxidation.

S1.7: H/D exchange reactions

The experimental conditions for the H/D exchange reactions of D₂O with 2,7-dimethyloctane, ethanol, propanal, acetone, tetrahydrofuran, methyl peroxide and hydrogen peroxide are shown in Table S1. The mass spectra in Figs. S11A-F show that only the *m/z* of ethanol and acetic acid is increased by one, after reacting with D₂O. Fig. S11G presents the mass peak of CH₃OOH and CH₃OOD, and Fig. S11H presents the mass peaks of H₂O₂, HDO₂ and D₂O₂. The measured photoionization efficiency spectra of CH₃OOD and CH₃OOH are very close to those measured in the literature (6). Similarly, the photoionization efficiency spectra of H₂O₂, HDO₂, and D₂O₂ are very similar to those of pure H₂O₂ (7).

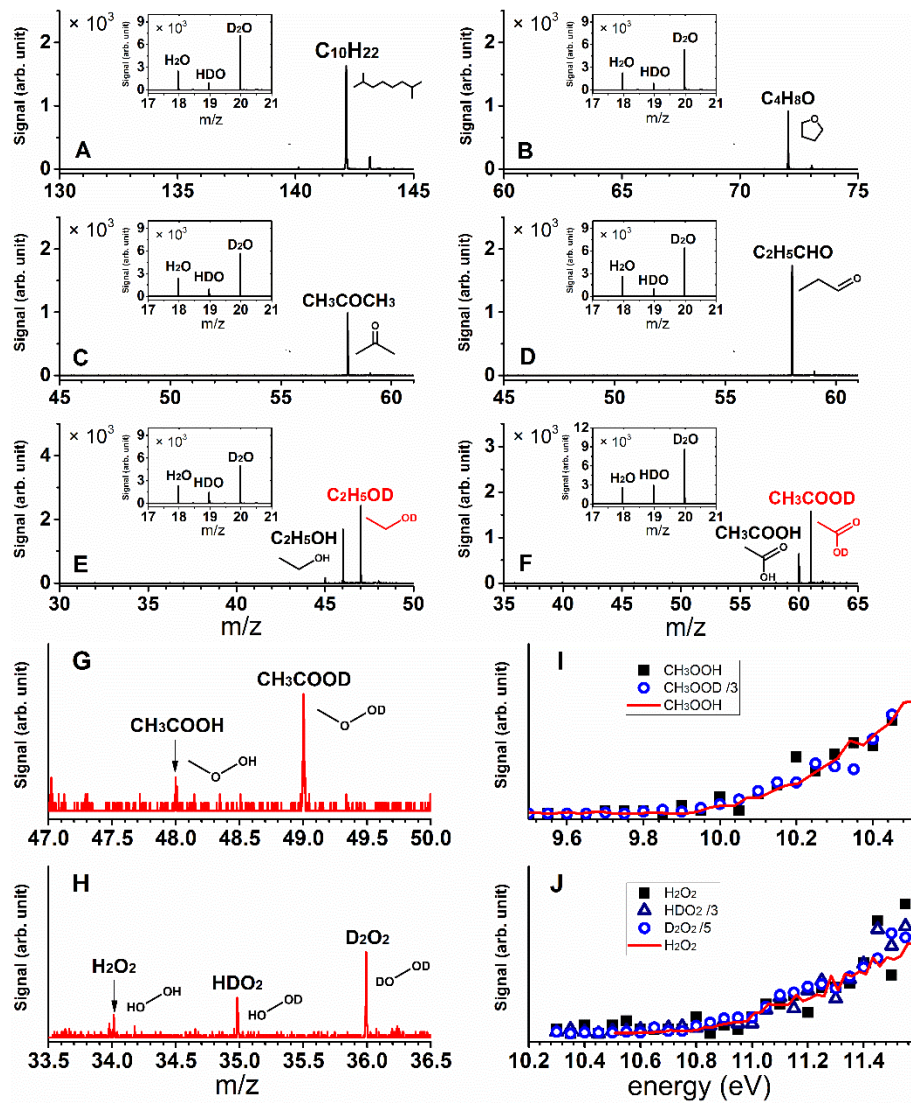


Figure S11: H/D exchange of alkane (A), cyclic ether (B), ketone (C), aldehyde (D), alcohol (E), acid (F), methylperoxide (G), and hydrogen peroxide (H) with D_2O at 530 K. Inset in A-F shows H/D exchange of H_2O and D_2O during each measurement. H_2O from background of reactor chamber. Methylperoxide and hydrogen peroxide produced during 2,7-dimethyloctane auto-oxidation (Table S1). Signal of CH_3OOD , HDO_2 , and D_2O_2 in (I) and (J) divided by 3, 3, and 5, respectively. Lines in (I) and (J) are PIE curves of methylperoxide (6) and hydrogen peroxide (7) in the literature.

S1.8: Fragments analysis of highly oxygenated intermediates

Table S2: Fragments from highly oxygenated intermediates in SVUV-PI-MBMS experiments with auto-oxidation of 13 organic compounds. Ions formed by elimination of -OOH, or through dissociation of the O-OH bond in the hydroperoxy group.

Organic compounds ($C_xH_yO_z$) ^a	$C_xH_{y-2}O_{z+3}$	$C_xH_{y-2}O_{z+3}$	$C_xH_{y-4}O_{z+4}$	$C_xH_{y-2}O_{z+5}$
Fragment pattern	break of -O-OH bond $C_xH_{y-3}O_{z+2}^+$	loss of -OOH $C_xH_{y-3}O_{z+1}^+$	loss of -OOH $C_xH_{y-5}O_{z+2}^+$	loss of -OOH $C_xH_{y-3}O_{z+3}^+$
2,7-dimethyloctane ($C_{10}H_{24}$)	$C_{10}H_{19}O_2^+$	$C_{10}H_{19}O^+$	$C_{10}H_{17}O_2^+$	$C_{10}H_{19}O_3^+$
cyclohexane (C_6H_{12})	$C_6H_9O_2^+$	$C_6H_9O^+$	$C_6H_7O_2^+$	$C_6H_9O_3^+$
<i>n</i> -heptane (C_7H_{16})	$C_7H_{13}O_2^+$	$C_7H_{13}O^+$	$C_7H_{11}O_2^+$	$C_7H_{13}O_3^+$
<i>n</i> -decane ($C_{10}H_{22}$)	$C_{10}H_{19}O_2^+$	$C_{10}H_{19}O^+$	$C_{10}H_{17}O_2^+$	$C_{10}H_{19}O_3^+$
<i>n</i> -dodecane ($C_{12}H_{26}$)	$C_{12}H_{23}O_2^+$	$C_{12}H_{23}O^+$	$C_{12}H_{21}O_2^+$	$C_{12}H_{23}O_3^+$
2-methylnonane ($C_{10}H_{22}$)	$C_{10}H_{19}O_2^+$	$C_{10}H_{19}O^+$	$C_{10}H_{17}O_2^+$	$C_{10}H_{19}O_3^+$
cycloheptane (C_7H_{14})	$C_7H_{11}O_2^+$	$C_7H_{11}O^+$	$C_7H_9O_2^+$	$C_7H_{11}O_3^+$
<i>n</i> -butylcyclohexane ($C_{10}H_{20}$)	$C_{10}H_{17}O_2^+$	$C_{10}H_{17}O^+$	$C_{10}H_{15}O_2^+$	$C_{10}H_{17}O_3^+$
1-decanol ($C_{10}H_{22}O$)	$C_{10}H_{19}O_3^+$	$C_{10}H_{19}O_2^+$	$C_{10}H_{17}O_3^+$	$C_{10}H_{19}O_4^+$
decanal ($C_{10}H_{20}O$)	$C_{10}H_{17}O_3^+$	$C_{10}H_{17}O_2^+$	$C_{10}H_{15}O_3^+$	$C_{10}H_{17}O_4^+$
2-decanone ($C_{10}H_{20}O$)	$C_{10}H_{17}O_3^+$	$C_{10}H_{17}O_2^+$	$C_{10}H_{15}O_3^+$	$C_{10}H_{17}O_4^+$
dipentyl ether ($C_{10}H_{22}O$)	$C_{10}H_{19}O_3^+$	$C_{10}H_{19}O_2^+$	$C_{10}H_{17}O_3^+$	$C_{10}H_{19}O_4^+$
methyl decanoate ($C_{11}H_{22}O_2$)	$C_{11}H_{19}O_4^+$	$C_{11}H_{19}O_3^+$	$C_{11}H_{17}O_4^+$	$C_{11}H_{19}O_5^+$

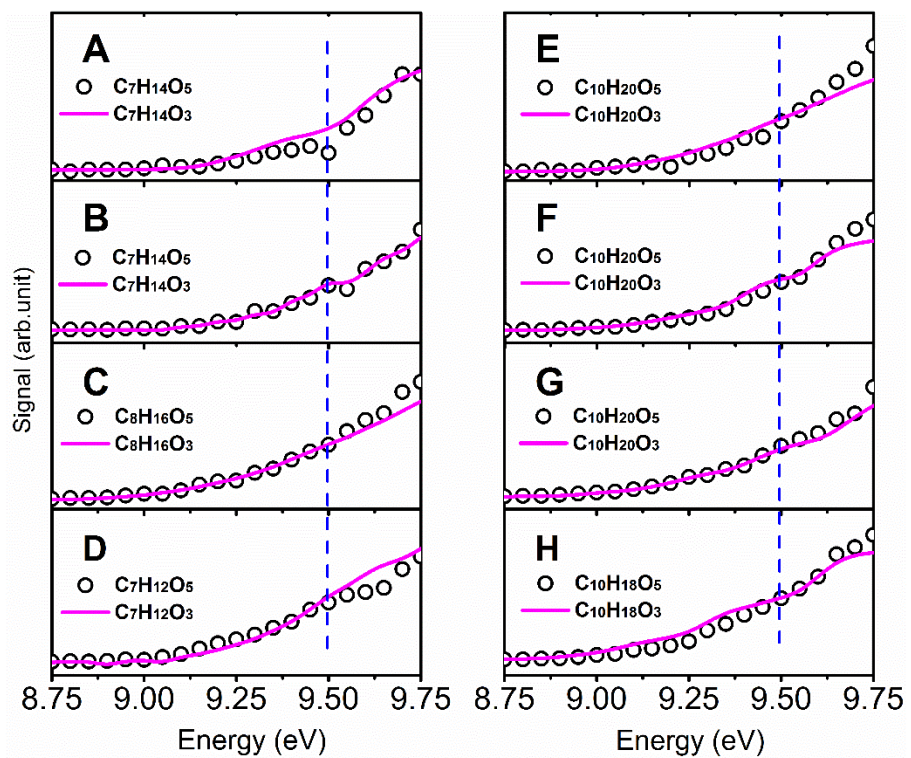
Note: ^a x equals to carbon number of organic compounds; y is equal to $2x+2$ for alkanes, alcohols, and ethers, $2x$ for cycloalkanes, aldehydes, ketone compounds, and esters; z is equal to 0 for hydrocarbons, 1 for alcohols, aldehydes, ketone compounds, and ethers, and 2 for esters.

S1.9: Relative ratio of $C_xH_{y-2}O_5$ to $C_xH_{y-2}O_3$

The total photoionization efficiency curve of $C_xH_{y-2}O_5$ and $C_xH_{y-2}O_3$ was obtained by including the signals of the parent ion and their fragments. Previous work of 2,5-dimethylhexane (8) shows that the dominant fragments are those occurring from the loss of –OOH, and the contribution from other fragments is less important at 9.5 eV. Here, focus was on the fragments from the loss of –OOH and the dissociation of O-OH bond in the hydroperoxy functional group. Neglecting the smaller fragments may increase the uncertainty of the relative ratios, but it will not affect our conclusions. For $C_xH_{y-2}O_3$ intermediates specifically, its total photoionization efficiency curve is the summation of the signal of $C_xH_{y-2}O_3$, $C_xH_{y-3}O$ (from the loss of -OOH), and $C_xH_{y-3}O_2$ (from the dissociation of O-OH bond in the hydroperoxy functional group). For the total photoionization efficiency curve of $C_xH_{y-2}O_5$ intermediates, only the summation of the signal of $C_xH_{y-2}O_5$ and $C_xH_{y-3}O_3$ (from the loss of -OOH) is considered. In most cases, the signal intensity of $C_xH_{y-3}O_4$ (from the dissociation of O-OH bond in the hydroperoxy functional group) is very low.

As shown in Fig. S12, the photoionization efficiency from 8.75 eV to 9.75 eV is very similar for $C_xH_{y-2}O_5$ and $C_xH_{y-2}O_3$, highly oxygenated intermediates produced from the oxidation of eight hydrocarbons. Note that loss of the ionized $C_xH_{y-2}O_3$ from the H atoms could also contribute to the signal of $C_xH_{y-3}O_3$, as well as the fragment of $C_xH_{y-2}O_5$ from the loss of –OOH. However, previous work on 2,5-dimethylhexane oxidation shows that the appearance energy of the dissociation products from the loss of the ionized $C_xH_{y-2}O_3$ in the H atoms is in the range of 10.3–12.7 eV (8), so it is unlikely that they contribute to the signal of $C_xH_{y-3}O_3$ below 9.75 eV.

Given the similar photoionization efficiency curve of $C_nH_{2n-2}O_5$ and $C_nH_{2n-2}O_3$, it is assumed that the ratio of the total photoionization cross section of $C_xH_{y-2}O_5$ to $C_xH_{y-2}O_3$ is the same at 9.5, or 9.6 eV, for all the hydrocarbons studied here. The relative ratios of $C_xH_{y-2}O_5$ to $C_xH_{y-2}O_3$ were then calculated from the total signal intensity of $C_xH_{y-2}O_5$ to $C_xH_{y-2}O_3$ at the temperature corresponding to their maximum formation. The total signal intensity of $C_xH_{y-2}O_5$ and $C_xH_{y-2}O_3$ was acquired using the same method used to determine the total photoionization efficiency curve. The photon energy was 9.5 eV for 2-methylhexane, 2-methylnonane, *n*-decane, 2,5-dimethylhexane, 2,7-dimethyloctane, cycloheptane, and *n*-butylcyclohexane auto-oxidation. In the case of *n*-heptane, the photon energy was 9.6 eV.



A: *n*-heptane; **B:** 2-methylhexane; **C:** 2,5-dimethylhexane

D: cycloheptane; **E:** *n*-decane; **F:** 2-methylnonane

G: 2,7-dimethyloctane; **H:** *n*-butylcyclohexane

Figure S12: Total photoionization efficiency curves of $\text{C}_x\text{H}_{y-2}\text{O}_5$ and $\text{C}_x\text{H}_{y-2}\text{O}_3$ from 8.75 to 9.75 eV for eight hydrocarbons. Blue lines mark signals at 9.5 eV. Data of 2-methylhexane and 2,5-dimethylhexane from Wang *et al.* (8, 9)

Section 2: Quantum chemistry calculation

S2.1: Detailed kinetic analysis of α,β -OOQOOH radical (A, B, and C in Figure 5) from *n*-decane and 2-methylnonane auto-oxidation

In this section, the kinetics for the EA and standard isomerization of α,β -OOQOOH radical was investigated (A, B, C in Fig. 5). The geometry of the reactants, products, and transition states were optimized at the B3LYP/6-31+G(d,p) level of theory and the total energy of all species were calculated at the same level of theory. The B3LYP/6-31+G(d,p) level of theory is a computationally affordable and economical method for the very large system (i.e., 14 or more heavy atoms) investigated in this work. The purpose of this kinetic analysis was to provide general insight into the effect of the type of C-H bond (e.g., primary, secondary, and tertiary) on the EA pathways. All values were calculated at standard state of 298 K and 1 bar. All calculations were performed using the Gaussian 09 software package (10). “j” stands for the radical site in the species. Figures S18-S20 show the lowest energy conformer of the three target reactants and their derived transition states (TS) and products. Detailed geometry parameters and frequencies are listed in Tables S5 and S6.

The standard enthalpies of formation for the TS structures in the ketohydroperoxide + OH pathways were calculated from those of the corresponding reactant and the energy difference between the TS structure and the reactant. The standard enthalpies of formation of the TS structures in the isomerization pathways were taken as an average from the energy difference between the TS and the reactant and the energy difference between the TS and the product. The enthalpy of formation for reactants (A, B, and C) and products (AP1, AP2, BP1, BP2, CP1, and CP2) were determined using the group additivity method (11). Tables S7 and S8 list the groups and their corresponding thermodynamic property values for target species.

Entropy and heat capacity contributions as a function of temperature were determined from the calculated structures; moments of inertia, vibrational frequencies, symmetry, electron degeneracy, number of optical isomers, and the known mass of each species were considered. The calculations used standard formulas from statistical mechanics for the contributions of translation, external rotation, and vibrations by using the SMCPs program (12). Contributions from internal rotors using Rotator (13) were substituted for contributions from the corresponding internal rotor torsion frequencies. Rotator is a program for the calculation of thermodynamic

functions from hindered rotations, with arbitrary potentials based on a method developed by Lay *et al.* This technique employs the expansion of the hindrance potential in the Fourier series, calculation of the Hamiltonian matrix based on wave functions of free internal rotation, and subsequent calculation of energy levels by direct diagonalization of the Hamiltonian matrix. Rotation barriers higher than 7 kcal/mol were treated as harmonic oscillators. Rotation barriers less than 7 kcal/mol, but higher than 0.5 kcal/mol, were treated as anharmonic oscillators. Rotation barriers less than 0.5 kcal/mol were treated as free rotors. Table S9 summarizes the considered reactions along with the corresponding energy barrier for each pathway.

The calculated ΔH^\ddagger and ΔS^\ddagger at 298 K for the EA and standard isomerization reactions of the A, B and C structures of the OOQOOH radical are presented in Fig. 5. First, for molecules A, B, and C, the activation energy difference between the EA channel and standard isomerization channel was -1.5, 1.0, and -3.0 kcal/mol, respectively. The activation energy differences from 300 to 800 K were close to those at 298 K (Figs. S13A, B, and C). Based on the calculated energy barriers, EA was favorable for molecules A and C, while standard isomerization was favorable for molecule B. In addition, for molecules A, B, and C, the entropy difference between the EA channel and standard isomerization channel was -0.7, 0.6, and 4.4 cal/mol/K, respectively. The entropy differences from 300 to 800 K were also close to those at 298 K (Figs. S13A', 2B', and 2C'). The entropy calculations indicated that EA was favorable for molecules B and C, while standard isomerization was favorable for molecule A. However, the entropy differences for molecules A and B were small and not expected to have a substantial effect on the rate constant. In summary: (1) EA of OOQOOH radicals A, B and C were feasible, and (2) EA of OOQOOH, by abstracting the tertiary C-H, were more favorable than EA by abstracting the primary and secondary C-Hs, because of the lower energy barrier and higher entropy difference of the transition state in the former.

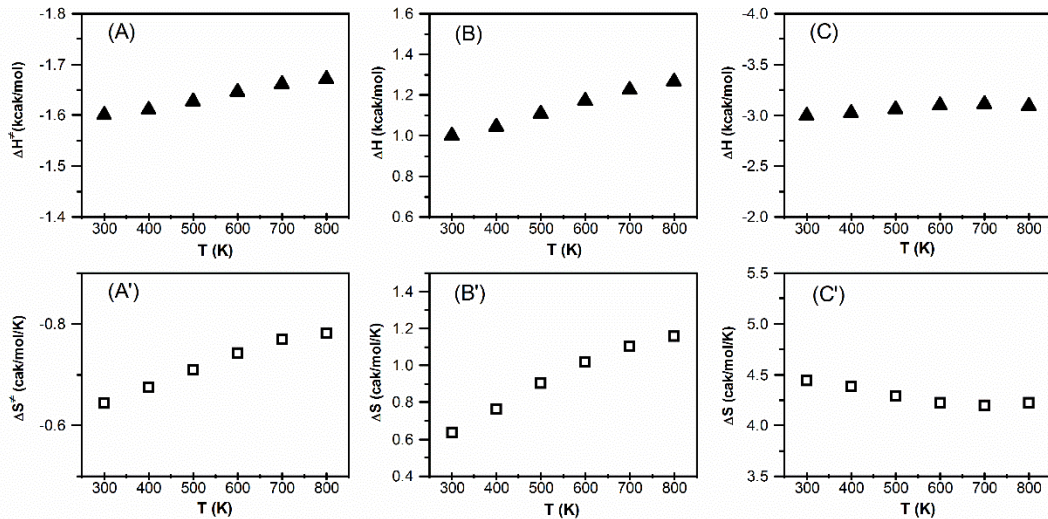


Figure S13: (A-C) activation energy difference between extensive auto-oxidation and standard isomerization for molecules A, B, and C in Fig. 5. The unit is kcal/mol. (A'-C') entropy difference between extensive auto-oxidation and standard isomerization for molecules A, B, and C in Fig. 5. The unit is cal/mol/K. The temperature range is 300-800 K.

Conversely, the equilibrium constant of the EA of the OOQOOH radical by abstracting at the tertiary C-H (molecule C in Fig. 5) is higher than that for secondary C-H (molecule A and B in Fig. 5), as shown in Fig. S14. The reason for this behavior is the higher stability of the P(OOH)₂ radical from the EA of OOQOOH by abstracting the tertiary C-H than that the P(OOH)₂ radicals with the radical site at primary and secondary carbons. Thus, in addition to kinetic favorability, the EA by abstracting the tertiary C-H of the OOQOOH radical is also thermodynamically favorable compared to its EA by abstracting the primary and secondary C-Hs. The aforementioned analysis is agreement with experimental observations in Fig. 4 of the manuscript. Kinetic analysis with pressure dependence was not performed in this work because pressure dependence was expected to be minimal for the very large system in Fig. 5, as a result of the large number of degrees of freedom. For example, the pressure dependence of the rate constant for the RO₂ isomerization in cyclohexane oxidation changed only within a factor of two between the high-pressure limit and the value at 1 bar in the temperature range of 500-800 K (14).

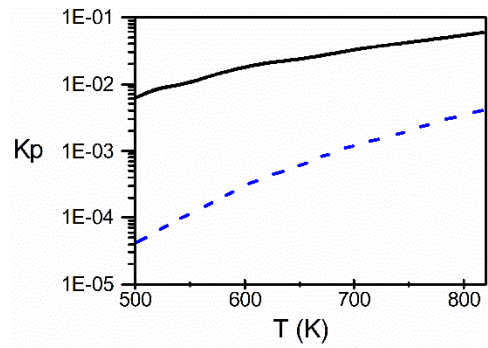


Fig. S14: Equilibrium constant of α,β -OOQOOH radical's extensive auto-oxidation by abstracting a tertiary C-H (molecule C in Fig. 5, solid line) and secondary C-H (molecule B in Fig. 5, dashed line).

S2.2: Potential energy surface of α,β -OOQOOH radical (E in Figure 5) in cyclohexane auto-oxidation

In this section, the potential energy surface for the α,β -OOQOOH radical was calculated (α is the position of the –OO group while γ is the position of the –OOH group), the most important OOQOOH radical in cyclohexane oxidation. Geometries and frequencies of reactant, products, and transition states of hydroperoxy-cyclohexylperoxy were characterized at the B3LYP/6-311++G(d,p) level of theory. The absence of imaginary frequencies verified that all stable structures were true minima at their respective levels of theory. Transition states are characterized as having only one negative eigenvalue of Hessian (force constant) matrices. Optimized geometries and calculated frequencies are presented in Tables S10 and S11. Single point energies of the optimized structures were calculated using the composite CBS-QB3 method (15). All calculations were performed using the Gaussian 09 software package (10).

Standard enthalpies of formation for each species in the potential energy diagram were determined by building isodesmic work reactions. Detailed information regarding work reactions and standard enthalpy of formation for the reference species are presented in Table S12.

Because it is the lowest among other cyclic conformers (16), the chair conformer was used here. Hydroperoxy and peroxy groups in hydroperoxy-cyclohexylperoxy can be in four different conformers: axial-axial, axial-equatorial, equatorial-axial and equatorial-equatorial, respectively. Theoretically, stereochemistry predicts the eq-eq conformer; it is the most stable conformer since the bulky groups point away from each other to avoid a steric effect. However, in this case, the ax-ax conformer was determined to be the most stable, the result of the hydrogen bonding effect between the hydroperoxy and peroxy group.

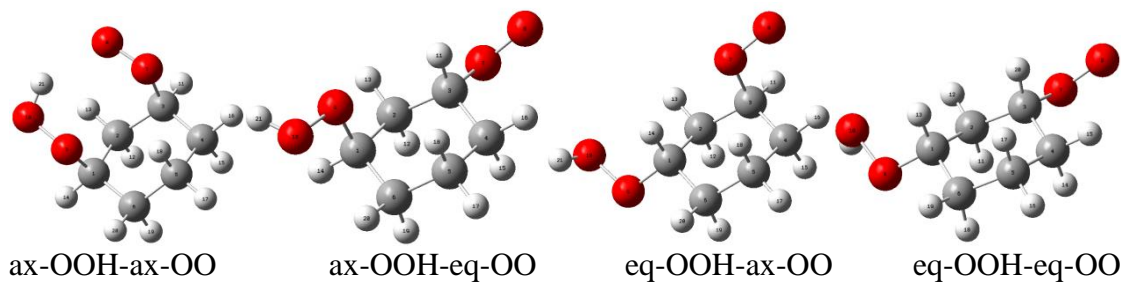


Figure S15: Optimized structures of four hydroperoxy-cyclohexylperoxy (α,γ -OOQOOH) conformers in cyclohexane auto-oxidation

Table S3: Relative total energies of hydroperoxy-cyclohexylperoxy (α,γ -OOQOOH) for different conformers in cyclohexane auto-oxidation at the CBS-QB3 level of theory

Conformers	Relative total energy in kcal mol ⁻¹
ax-OOH-cyclohexyl-ax-OO	0
ax-OOH-cyclohexyl-eq-OO	0.9
eq-OOH-cyclohexyl-ax-OO	1.0
eq-OOH-cyclohexyl-eq-OO	1.5

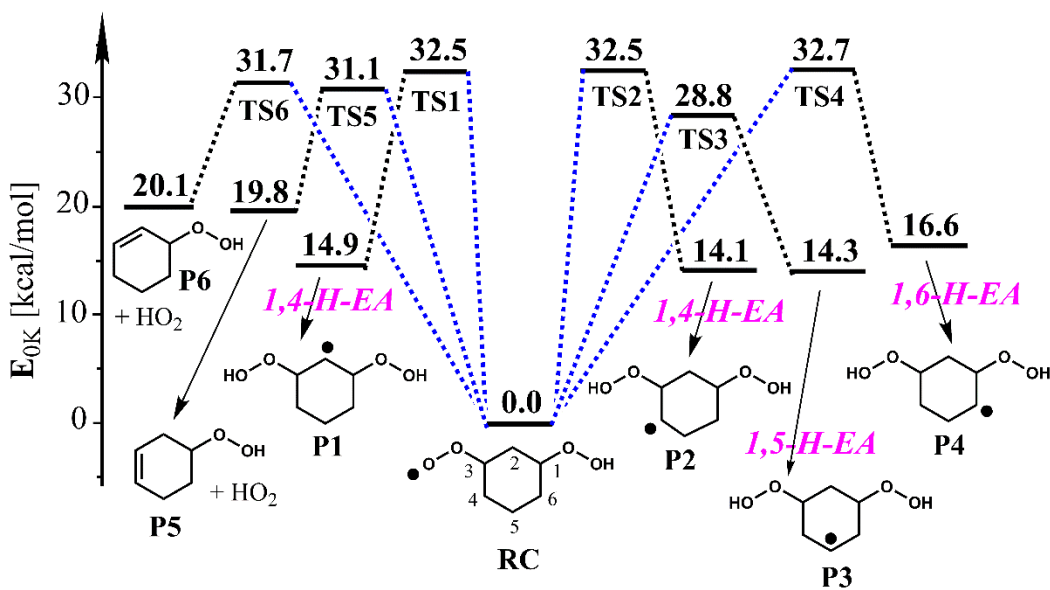
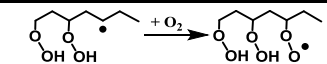
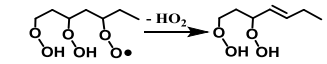
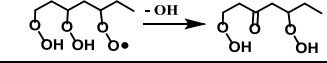
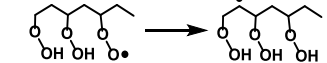
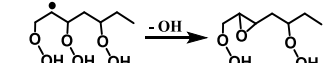
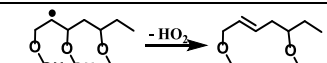
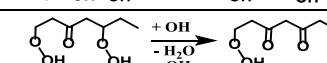
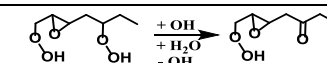
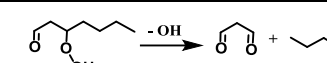


Figure S16: Potential energy surface of ax-hydroperoxy-cyclohexyl-ax-peroxy (ax-OOH-ax-OO) from cyclohexane auto-oxidation. (EA: extensive auto-oxidation)

Section 3: Kinetic modeling for third O₂ addition pathways

Third O₂ addition pathways, and subsequent reactions leading to C₇H₁₄O₅ (keto-dihydroperoxide and dihydroperoxy cyclic ether), were incorporated with C₇H₁₂O₄ (diketo-hydroperoxide and keto-hydroperoxy cyclic ether) species, into a recent *n*-heptane kinetic model (17). The rate rules utilized for the third O₂ addition reaction mechanism (9) are shown in Table S4. Simulations were performed at 1 bar and 50 bar, equivalence ratio of 0.5, and in a temperature range from 575 K-800 K with the homogenous batch reactor in the CHEMKIN PRO software (18). The composition of the unburnt mixture was 0.02 heptane/ 0.44 O₂/ 0.54 N₂. The addition of third O₂ addition pathways in the *n*-heptane model decreased ignition delay times. Results in Fig. S17 reveal that (i) the effect of third O₂ addition pathways on the ignition delay time was more evident at lower temperatures; (ii) the effect of third O₂ addition pathways on the ignition delay time was more apparent at higher pressures; correspondingly, the ratio of 5O to 3O species was higher at higher pressure. For example, a reduction of the ignition delay time of about 20% was noted at 1 bar, and of 60% at 50 bar, at a temperature of 600 K.

Table S4: Rate rules utilized for the third O₂ addition reaction mechanism in *n*-heptane kinetic model.

Reactions	Reaction type	Analogous Reaction	Example
O ₂ +P(OOH) ₂ = OOP(OOH) ₂	O ₂ addition	O ₂ +QOOH = OOQOOH	
OOP(OOH) ₂ = ODHP+HO ₂	Concerted elimination	OOQOOH = OHP+HO ₂	
OOP(OOH) ₂ = KDHP+OH	H-migration, β-scission	OOQOOH = KHP+OH	
OOP(OOH) ₂ = T(OOH) ₃	H-migration	OOQOOH = P(OOH) ₂	
T(OOH) ₃ = DHPCE+OH	Cyclization	P(OOH) ₂ = HPCE+OH	
T(OOH) ₃ = ODHP+HO ₂	C-O β-scission	P(OOH) ₂ = OHP+HO ₂	
KDHP+OH = H ₂ O+OH+ DKHP	H-abstraction, β-scission	KHP + OH = H ₂ O+OH+DKET	
DHPCE+OH = H ₂ O+OH+KHPCE	H-abstraction, β-scission	KHP + OH = H ₂ O+OH+DKET	
ODHP, KDHP, DHPCE, DKHP, and KHPCE decomposition	-OOH dissociation	KHP = products	

Note: ODHP: olefinic dihydroperoxide; KDHP: keto-dihydroperoxide; DHPCE: dihydroperoxy cyclic ether; DKHP: diketo-hydroperoxide; KHPCE: keto-hydroperoxy cyclic ether; KHP: keto-hydroperoxide; DKET: diketo compound

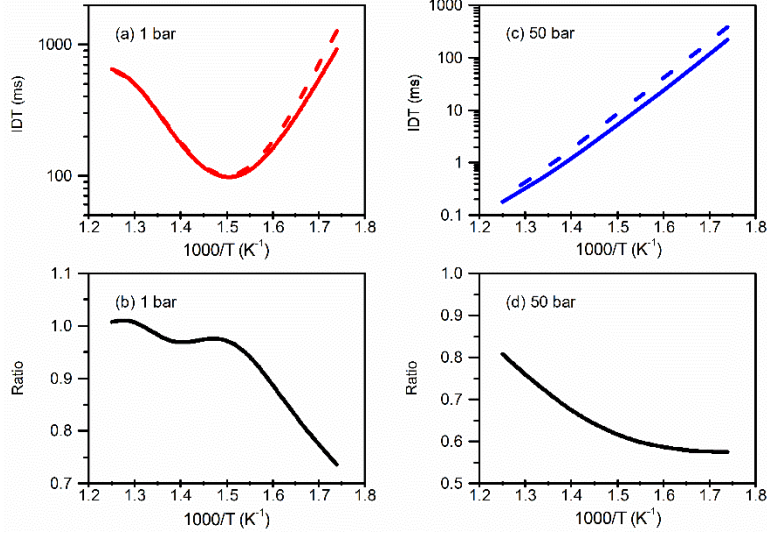


Figure S17: Ignition delay times for *n*-heptane/O₂/N₂ mixtures at $\phi = 0.5$ and 50 bar. (a) Red dashed line and red solid line indicate ignition delay times obtained by simulation without third O₂ addition reactions and simulation with third O₂ addition reactions at 1 bar, respectively; (b) ratio of ignition delay time with third O₂ addition reactions to ignition delay time without third O₂ addition reactions at 1 bar. (c) Blue dashed line and blue solid line indicate ignition delay times obtained by simulation without third O₂ addition reactions and simulation with third O₂ addition reactions at 50 bar, respectively; (d) ratio of ignition delay time with third O₂ addition reactions to ignition delay time without third O₂ addition reactions at 50 bar.

Section 4: Supporting information for quantum chemistry calculation

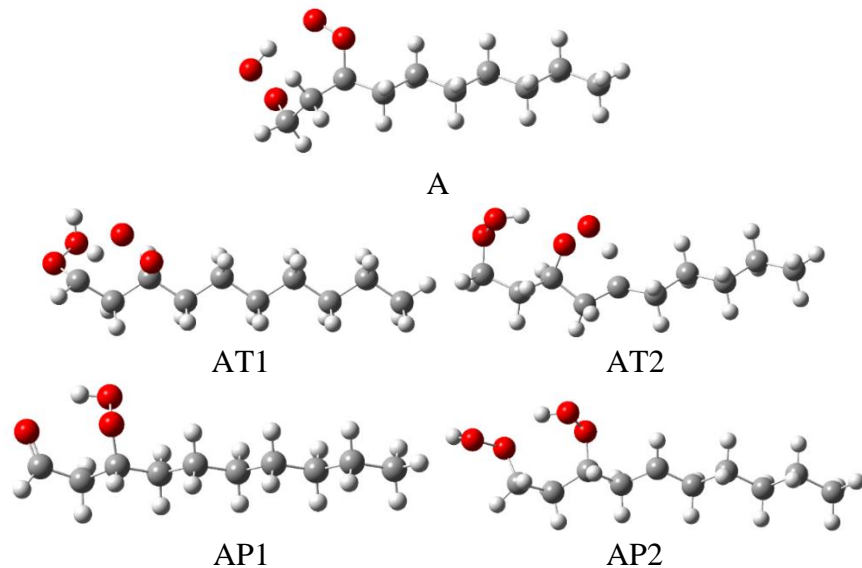


Figure S18: Lowest energy conformer of target species A ($C_{10}H_{21}O_4$. 1-OOH-3-OOj-decane), AT1 ($C_{10}H_{21}O_4$), AT2 ($C_{10}H_{21}O_4$), AP1 ($C_{10}H_{20}O_3$. 1-CHO-3-OOH-decane), and AP2 ($C_{10}H_{21}O_4$. 1-OOH-3-OOH-5j-decane). A \rightarrow AT1 \rightarrow AP1 is standard isomerization; A \rightarrow AT2 \rightarrow AP2 is extensive auto-oxidation.

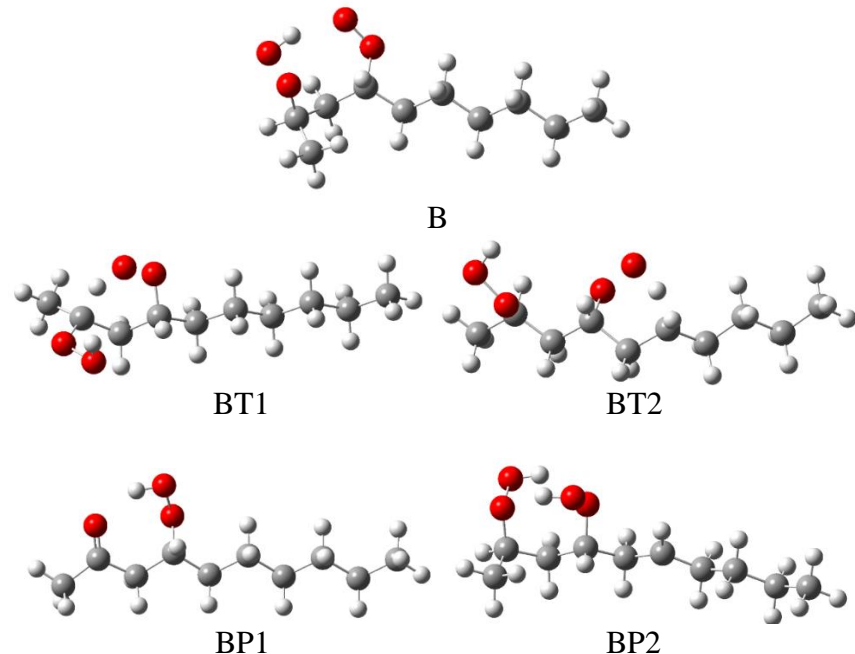


Figure S19: Lowest energy conformer of target species B ($C_{10}H_{21}O_4$. 2-OOH-4-OOj-decane), BT1 ($C_{10}H_{21}O_4$), BT2 ($C_{10}H_{21}O_4$), BP1 ($C_{10}H_{20}O_3$. 2-CO-4-OOH-decane), BP2 ($C_{10}H_{21}O_4$. 2-OOH-4-OOH-6j-decane). B \rightarrow BT1 \rightarrow BP1 is standard isomerization; B \rightarrow BT2 \rightarrow BP2 is extensive auto-oxidation.

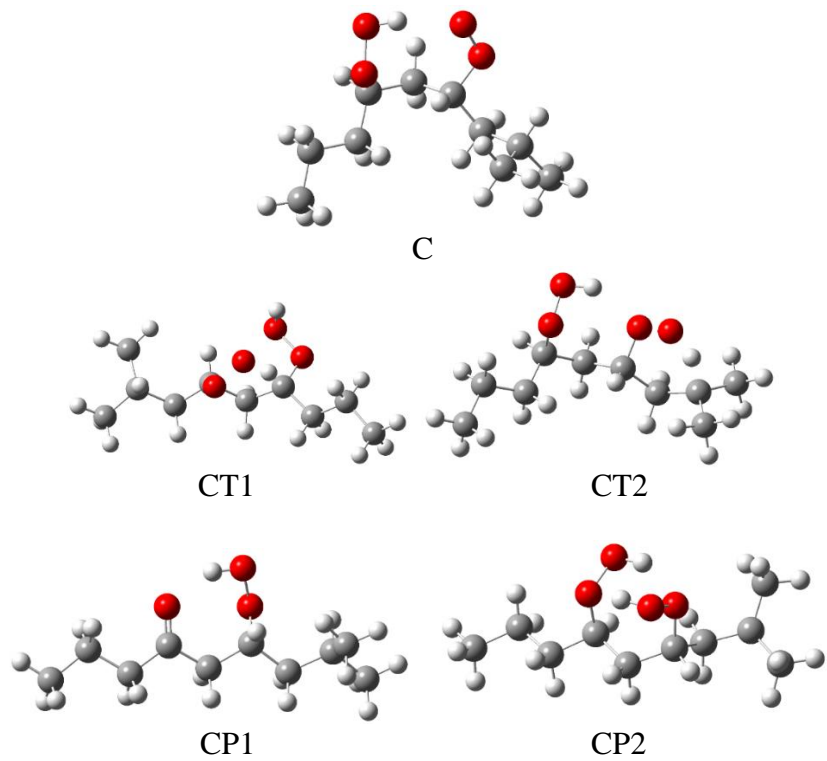


Figure S20: Lowest energy conformer of target species C ($C_{10}H_{21}O_4$. 4-OOj-6-OOH-isodecane), CT1 ($C_{10}H_{21}O_4$), CT2 ($C_{10}H_{21}O_4$), CP1 ($C_{10}H_{20}O_3$. 4-OOH-6-CO-isodecane), CP2 ($C_{10}H_{21}O_4$. 2j-4-OOH-6-OOH-isodecane). C→CT1→CP1 is standard isomerization; C→CT2→CP2 is extensive auto-oxidation.

Table S5: Cartesian coordinates for α,γ -OOQOOH radical A, B, and C in Fig. 5, and derived transition states and products at the B3LYP/6-31+G(d,p) level of theory.

Compound	Atom	x	y	z
A	C	-3.93733300	-1.51290800	-0.09038000
	H	-4.81841900	-1.94380600	0.40081100
	H	-3.36629400	-2.32375900	-0.56030300
B	C	-3.08718300	-0.73577500	0.92235700
	H	-3.72426700	-0.00252000	1.42417000
	H	-2.73745100	-1.42990200	1.69599400
	C	-1.89575600	-0.01056100	0.27221000
	H	-1.99208000	-0.02161300	-0.81833000
	C	-0.52210000	-0.50281900	0.71314100
	H	-0.51122100	-1.59130100	0.56502400
	H	-0.42045700	-0.33910900	1.79482400
	C	0.65605600	0.13233200	-0.03745300
	H	0.63075600	1.22052500	0.09834500
	H	0.53555900	-0.04772600	-1.11524700
	C	2.01772700	-0.40706600	0.42000900
	H	2.04352100	-1.49818300	0.28316000
	H	2.13235300	-0.23191100	1.49951300
	C	3.20231800	0.22474700	-0.32289800
	H	3.17261400	1.31550100	-0.18761100
	H	3.08876800	0.04853900	-1.40240700
	C	4.56763400	-0.30476900	0.13491600
	H	4.59933400	-1.39575800	-0.00181700
	H	4.68104200	-0.13001800	1.21493100
	C	5.75234400	0.33036200	-0.60524500
	H	5.71993300	1.42026600	-0.46927100
	H	5.64021000	0.15476300	-1.68418000
C	C	7.11299800	-0.20160700	-0.14083200
	H	7.18997100	-1.28410200	-0.29824500
	H	7.93565400	0.27283400	-0.68667700
	H	7.26896700	-0.01107200	0.92768900
	O	-4.33838100	-0.72692600	-1.20906000
	O	-5.22982100	0.31505500	-0.72728100
	H	-4.60204500	1.06110000	-0.63307600
	O	-1.93199500	1.43017600	0.63235000
	O	-2.95813800	2.06739900	0.09871000
AP1	C	-4.81080400	-0.64194400	0.23438800
	H	-5.28696900	-1.29969900	0.99044200
	C	-3.48675000	-1.08833200	-0.33743000
	H	-3.38373400	-2.17496800	-0.24644700
	H	-3.45678100	-0.81780700	-1.39744200
	C	-2.28749300	-0.41516400	0.38475500
	H	-2.22284600	-0.78943900	1.41647300
	C	-0.96583900	-0.67560600	-0.34489700
	H	-1.02068200	-0.19948400	-1.33111100
	H	-0.87635600	-1.75729700	-0.51768100
	C	0.26377000	-0.16762200	0.41823000
	H	0.31072900	-0.65877300	1.40144000
	H	0.14459100	0.90462200	0.61320400
	C	1.57882400	-0.41367100	-0.33317300
	H	1.53528800	0.08671400	-1.31115900
	H	1.68478600	-1.48818500	-0.54429200
	C	2.81724600	0.07460600	0.43017300

	H	2.85889600	-0.42439800	1.40942300
	H	2.71177400	1.14865600	0.64009000
	C	4.13523900	-0.16847400	-0.31677100
	H	4.09564800	0.33225800	-1.29524600
	H	4.23996400	-1.24278200	-0.52898500
	C	5.37447300	0.31682900	0.44731600
	H	5.41408900	-0.18278700	1.42529500
	H	5.27076000	1.39026900	0.65799100
	C	6.68694800	0.06931200	-0.30527200
	H	6.69145600	0.58442600	-1.27328100
	H	7.55014500	0.42790000	0.26598300
	H	6.83703400	-0.99953900	-0.49921500
	O	-5.35202800	0.40366500	-0.07854400
	O	-2.52702100	0.97740100	0.62075600
	O	-2.76889500	1.64125900	-0.65235700
	H	-3.74792500	1.64211200	-0.65824500
AP2	C	-4.13586000	-0.85448200	0.68272100
	H	-3.99750700	-0.35160000	1.64703400
	H	-4.80289500	-1.71385600	0.81872800
	C	-2.80404000	-1.29757800	0.07737400
	H	-2.49261700	-2.18174300	0.64907500
	H	-2.96921400	-1.63114000	-0.95498100
	C	-1.64328400	-0.28722400	0.10816500
	H	-1.47744100	0.07142000	1.13215000
	C	-0.34758000	-0.90786100	-0.43955500
	H	-0.51139000	-1.13538600	-1.51047000
	H	-0.19670700	-1.88426500	0.04421900
	C	0.86351400	-0.05184000	-0.25565000
	H	0.72872600	1.02734800	-0.26989900
	C	2.23818300	-0.61614800	-0.41375200
	H	2.43041500	-0.84970100	-1.47988000
	H	2.30248700	-1.58892300	0.10080900
	C	3.35789200	0.30721600	0.09236200
	H	3.18592200	0.52916800	1.15447300
	H	3.29495400	1.26879000	-0.43606500
	C	4.76248200	-0.28196500	-0.08665000
	H	4.93132700	-0.50456500	-1.15065600
	H	4.82132300	-1.24675700	0.43872300
	C	5.88377200	0.63488400	0.41998000
	H	5.71287400	0.86130400	1.48160300
	H	5.83038800	1.59665900	-0.10865900
	C	7.28338500	0.03386500	0.24597900
	H	7.49794500	-0.17182300	-0.80958200
	H	8.05958300	0.71211100	0.61684600
	H	7.37881900	-0.91188500	0.79280100
	O	-4.75757100	0.06040700	-0.23643400
	O	-5.99056200	0.51656500	0.39733200
	H	-6.63699700	0.26318600	-0.28238400
	O	-1.88299600	0.86039900	-0.72019800
	O	-2.65331100	1.83901800	0.02612300
	H	-3.56526800	1.55734800	-0.19431600
AT1	C	-4.23815200	0.38097300	-0.40633400
	H	-3.82230700	-0.91160600	-0.48505200
	H	-4.99655800	0.52786900	-1.18019900
	C	-2.89948700	1.06666400	-0.55807800
	H	-2.75878500	1.32978800	-1.61151900

	H	-2.87627900	1.99308400	0.03104800
	C	-1.72538600	0.15153900	-0.11783400
	H	-1.80972300	-0.06598200	0.95543700
	C	-0.35414800	0.73331500	-0.45155800
	H	-0.31170600	1.74609200	-0.02846200
	H	-0.27645800	0.84606000	-1.54136100
	C	0.82253800	-0.09874100	0.07661200
	H	0.76896900	-1.10809600	-0.34805700
	H	0.72210300	-0.21517500	1.16512200
	C	2.18712700	0.52525500	-0.24350000
	H	2.23700000	1.53606900	0.18780700
	H	2.28160600	0.65300800	-1.33165600
	C	3.37175000	-0.30313700	0.27139200
	H	3.32553200	-1.31026000	-0.16722400
	H	3.27295400	-0.43955800	1.35815600
	C	4.73888900	0.32143500	-0.03705900
	H	4.78659800	1.32755900	0.40504300
	H	4.83748200	0.46164700	-1.12354000
	C	5.92416300	-0.50922500	0.47284600
	H	5.87895600	-1.51319100	0.02849100
	H	5.82452000	-0.65194100	1.55788300
	C	7.28610400	0.12360000	0.16478400
	H	7.37585800	1.11488200	0.62502500
	H	8.10884500	-0.49355500	0.54190900
	H	7.43067600	0.24656700	-0.91524400
	O	-4.73418000	0.58564700	0.87555700
	O	-6.03173900	-0.06214100	0.97249900
	H	-5.82156000	-0.79118900	1.58187500
	O	-1.84658100	-1.08500200	-0.83440900
	O	-2.99476400	-1.76752000	-0.35528500
AT2	C	4.58956900	0.61308400	0.00446700
	H	5.38170000	0.80394100	0.74021400
	H	4.83128800	1.15521000	-0.91848700
	C	3.23208500	1.06475200	0.56063700
	H	3.10707900	0.71429800	1.59126400
	H	3.23550500	2.16107300	0.60258200
	C	2.02374300	0.60049100	-0.25365900
	H	2.25123500	0.55752600	-1.32638200
	C	0.75000200	1.44475700	-0.00279700
	H	0.92307300	2.44575500	-0.42521100
	H	0.62628500	1.56001900	1.08091800
	C	-0.49363000	0.82044100	-0.60689100
	H	-0.05102300	-0.46625500	-0.69356500
	H	-0.62620600	1.03103400	-1.67389700
	C	-1.77366600	0.84230200	0.19730900
	H	-2.06130600	1.89537900	0.36828200
	H	-1.58126800	0.42426300	1.19548100
	C	-2.94593700	0.10349700	-0.46316000
	H	-2.66305100	-0.94490000	-0.62958700
	H	-3.13070200	0.53455400	-1.45752600
	C	-4.23791600	0.15710800	0.36230400
	H	-4.51526600	1.20705700	0.53767600
	H	-4.05200300	-0.27903900	1.35455300
	C	-5.41675400	-0.57223200	-0.29568000
	H	-5.13847900	-1.61991800	-0.47434000
	H	-5.60594100	-0.13382400	-1.28538600

	C	-6.70161200	-0.52060800	0.53886000
	H	-7.02491000	0.51386800	0.70560700
	H	-7.52217800	-1.04926600	0.04202000
	H	-6.55449400	-0.98372600	1.52175600
	O	4.63569400	-0.74311700	-0.42253600
	O	4.41295700	-1.58960300	0.73836500
	H	3.45889400	-1.77399500	0.63121900
	O	1.73012900	-0.74279000	0.18384400
	O	0.79077800	-1.30881500	-0.71661400
B	C	-2.67847900	2.44855800	-0.29040000
	H	-1.77891100	2.28315600	-0.89224600
	H	-2.40875300	3.06362400	0.57392300
	H	-3.39609800	3.00283200	-0.90090300
	C	-3.29245500	1.13143700	0.18022800
	H	-4.20726200	1.33378900	0.75285200
	C	-2.35997000	0.26696500	1.05170100
	H	-2.94034700	-0.57240600	1.44354700
	H	-2.03938000	0.85673600	1.91849800
	C	-1.13712700	-0.28315500	0.29670100
	H	-1.25073300	-0.13008900	-0.78125800
	C	0.21306500	0.22300600	0.79331300
	H	0.33989800	-0.08746000	1.83963500
	H	0.15876600	1.31950500	0.80402500
	C	1.41553100	-0.22723800	-0.04709600
	H	1.26988600	0.09729200	-1.08737900
	H	1.45647100	-1.32316000	-0.06874200
	C	2.74870800	0.32365600	0.47606900
	H	2.89032300	0.00027200	1.51747900
	H	2.70465700	1.42249000	0.50094300
	C	3.95960400	-0.11504700	-0.35777700
	H	3.81913500	0.20762300	-1.39973100
	H	4.00359000	-1.21346500	-0.38260400
	C	5.29518500	0.43185800	0.16361400
	H	5.43619200	0.10857900	1.20435700
	H	5.25093000	1.52962900	0.18877000
	C	6.49954200	-0.01074200	-0.67521700
	H	6.40382600	0.32566000	-1.71442700
	H	7.43506800	0.39792100	-0.27830300
	H	6.59291400	-1.10311500	-0.68873200
	O	-3.66145900	0.45658900	-1.03029400
	O	-4.44617900	-0.71550400	-0.68470400
	H	-3.75655800	-1.41084600	-0.70889100
	O	-1.07783900	-1.75983900	0.45606300
	O	-2.06017800	-2.38679000	-0.16452000
BP1	C	5.04999500	-1.35917300	-0.15930300
	H	4.98428000	-1.97346500	-1.06626900
	H	4.99099000	-2.04203500	0.69501300
	H	6.00495500	-0.83168300	-0.15611700
	C	3.90784100	-0.36435400	-0.14691900
	C	2.52888400	-0.92863800	0.15704100
	H	2.53973100	-1.22519000	1.21679900
	H	2.41682100	-1.86610300	-0.40520400
	C	1.31586500	-0.01680900	-0.09329500
	H	1.31308300	0.34250300	-1.12856800
	C	-0.00105900	-0.74223800	0.21206300
	H	-0.02910400	-0.97084600	1.28677100

	H	0.00195600	-1.70787700	-0.31248600
	C	-1.24715700	0.05973700	-0.18162800
	H	-1.22565500	0.25191900	-1.26398700
	H	-1.20710300	1.03959100	0.30761200
	C	-2.55766700	-0.65031100	0.18248200
	H	-2.57840200	-0.83768300	1.26602300
	H	-2.58597300	-1.63946000	-0.29865400
	C	-3.81112000	0.13998700	-0.21589300
	H	-3.79345400	0.32704700	-1.29960300
	H	-3.78248300	1.12897200	0.26362500
	C	-5.12471800	-0.56229100	0.15294800
	H	-5.14236300	-0.74895100	1.23578300
	H	-5.15364700	-1.55055900	-0.32699100
	C	-6.37148200	0.23542700	-0.24671600
	H	-6.40175900	0.40699600	-1.32935800
	H	-7.29074100	-0.29100900	0.03246300
	H	-6.38735500	1.21611900	0.24340700
	O	4.11518700	0.82093600	-0.37238500
	O	1.37365500	1.13786000	0.76356000
	O	1.81425300	2.29451400	0.00715600
	H	2.76517300	2.07720500	-0.11159100
BP2	C	3.63978500	1.41866500	1.47268500
	H	2.90373400	0.95634400	2.13702000
	H	3.47232700	2.50021100	1.47299100
	H	4.63792500	1.22624100	1.87544200
	C	3.53324800	0.88655400	0.04466500
	H	4.29071700	1.37119200	-0.58455500
	C	2.16084300	1.08799300	-0.62088100
	H	2.25113400	0.86004700	-1.68910100
	H	1.92739500	2.15858600	-0.55724400
	C	0.97012400	0.29708600	-0.05536900
	H	0.81604000	0.49825900	1.00875400
	C	-0.32609200	0.58911300	-0.82489200
	H	-0.18634700	0.24234600	-1.86700500
	H	-0.44812300	1.68018600	-0.90012800
	C	-1.54503700	-0.02642100	-0.21785400
	H	-1.42196000	-0.94883800	0.34560800
	C	-2.91440100	0.37068500	-0.66532500
	H	-3.10195900	-0.01333400	-1.68771600
	H	-2.97162200	1.46697700	-0.76380400
	C	-4.04214900	-0.12267900	0.25509700
	H	-3.88333000	0.27983800	1.26500400
	H	-3.97684600	-1.21601200	0.34725000
	C	-5.44373400	0.26269700	-0.23421400
	H	-5.59893200	-0.14337900	-1.24358800
	H	-5.50486700	1.35562300	-0.33298800
	C	-6.56346500	-0.22819000	0.69057900
	H	-6.45671000	0.19010400	1.69848800
	H	-7.55003600	0.06159300	0.31292200
	H	-6.55012200	-1.32066900	0.78318700
	O	3.90633100	-0.50795600	0.15794900
	O	3.90580200	-1.11698800	-1.15987800
	H	2.98262600	-1.44377900	-1.20232800
	O	1.19903300	-1.13389300	-0.17534500
	O	1.61101700	-1.67569100	1.10762500
	H	2.57676500	-1.49833500	1.07204200

BT1	C	-4.41183800	1.49578200	-0.29947000
	H	-4.69636600	1.65775300	-1.34794600
	H	-3.89868300	2.39197300	0.05997500
	H	-5.32170200	1.35303100	0.28936900
	C	-3.48763100	0.30452700	-0.17033700
	H	-3.01102800	0.26657800	1.08390200
	C	-2.15962800	0.34160300	-0.92148800
	H	-1.99551800	1.36381500	-1.27971900
	H	-2.21695300	-0.32466300	-1.79003500
	C	-0.94093700	-0.06027600	-0.05318400
	H	-0.97160500	-1.13615400	0.15383700
	C	0.39288500	0.33825000	-0.67979900
	H	0.42203300	1.43236300	-0.77438900
	H	0.41213200	-0.06391000	-1.70187300
	C	1.62335600	-0.15375000	0.09437400
	H	1.58326700	-1.24901300	0.17940600
	H	1.58478100	0.23733800	1.11794500
	C	2.94613200	0.25740300	-0.56541400
	H	2.97662500	1.35239600	-0.66314700
	H	2.98322800	-0.14121100	-1.59014200
	C	4.18642900	-0.21357300	0.20531100
	H	4.15766100	-1.30839000	0.30659300
	H	4.15013400	0.18751600	1.22855500
	C	5.51121200	0.19719600	-0.45117300
	H	5.53830900	1.29078200	-0.55588900
	H	5.54941300	-0.20748800	-1.47219600
	C	6.74512100	-0.27067000	0.32915500
	H	6.76450800	-1.36313600	0.42167500
	H	7.67260200	0.03762100	-0.16555800
	H	6.75392600	0.14680100	1.34304400
	O	-4.27882000	-0.84112100	-0.34757200
	O	-3.45182000	-2.03467300	-0.31724600
	H	-3.55839100	-2.31188700	0.61009700
	O	-1.03882400	0.63831700	1.20043900
	O	-2.14415800	0.10859500	1.91670900
BT2	C	4.64441600	-1.14579700	0.82598000
	H	4.84308600	-1.91365600	0.07030000
	H	4.39431400	-1.64043400	1.77100400
	H	5.55443100	-0.55992300	0.97483900
	C	3.49916600	-0.24012800	0.38555800
	H	3.27508000	0.50116300	1.16245700
	C	2.22692100	-1.01973600	0.03326600
	H	2.00238300	-1.70384100	0.86036800
	H	2.42258700	-1.63777400	-0.85160700
	C	1.00284100	-0.14816000	-0.23739000
	H	1.23791000	0.64182200	-0.96027300
	C	-0.22942000	-0.95865200	-0.71205900
	H	-0.36318700	-1.80710300	-0.02990900
	H	-0.00238500	-1.36497600	-1.70891900
	C	-1.49215400	-0.11994200	-0.75278900
	H	-1.59675500	0.48844400	-1.65788700
	H	-1.10018300	0.86081400	0.12714100
	C	-2.78254900	-0.73594500	-0.26229600
	H	-2.62620200	-1.15256600	0.74280800
	H	-3.02628400	-1.60056600	-0.90599400
	C	-3.97593900	0.22924200	-0.24756700

	H	-4.12514800	0.63673500	-1.25788400
	H	-3.73815500	1.08629600	0.39761500
	C	-5.27897100	-0.42217300	0.23355100
	H	-5.12765300	-0.82808400	1.24328200
	H	-5.51344700	-1.28231600	-0.40924800
	C	-6.46850100	0.54446400	0.24555300
	H	-6.66610000	0.94218900	-0.75694600
	H	-7.38160500	0.04918500	0.59276500
	H	-6.27946300	1.39694200	0.90847200
	O	3.82813200	0.46731900	-0.82800000
	O	4.88730500	1.41785000	-0.52154100
	H	4.40034700	2.25519100	-0.59898500
	O	0.65642700	0.47357000	1.01020200
	O	-0.30416900	1.48294000	0.74130800
C	C	3.94254500	-1.83682500	-0.49939500
	H	4.34167400	-1.39873900	-1.42115800
	H	3.44370800	-2.77810300	-0.76401100
	H	4.79064100	-2.08219100	0.14878900
	C	2.96998400	-0.87733300	0.20432700
	H	3.51714700	0.04638800	0.43462800
	C	1.81247300	-0.51573400	-0.74994600
	H	1.20609200	-1.41188100	-0.94115500
	H	2.21957600	-0.20861100	-1.72289200
	C	0.85703800	0.57437800	-0.27469400
	H	0.49147500	0.39191800	0.73903200
	C	-0.32211500	0.85835200	-1.22248600
	H	-0.20876600	0.29308600	-2.15495900
	H	-0.30286800	1.91657600	-1.49643300
	C	-1.70411300	0.54437400	-0.61382500
	H	-2.47444800	0.95083000	-1.28392000
	C	-1.96800500	-0.94770200	-0.37840100
	H	-1.25951400	-1.33102800	0.36865600
	H	-1.74641300	-1.47282000	-1.31762900
	C	-3.40303100	-1.26955900	0.06188700
	H	-4.10309200	-0.87517600	-0.68713800
	H	-3.62071500	-0.74066100	0.99564200
	C	-3.64073900	-2.77251800	0.24503500
	H	-2.97670100	-3.18902100	1.01189600
	H	-4.67123800	-2.97487300	0.55521100
	H	-3.45968100	-3.32376700	-0.68582400
	C	2.47406000	-1.48219500	1.52752800
	H	1.83274500	-0.79434300	2.08824300
	H	1.90516900	-2.40390900	1.34889300
	H	3.31930900	-1.73615500	2.17606000
	O	1.69796100	1.79487600	-0.14945900
	O	1.09174300	2.77657300	0.49260600
	O	-1.85963000	1.15980400	0.67211900
	O	-1.85906500	2.60166200	0.49916400
	H	-0.92076700	2.80773500	0.69245300
CP2	C	3.72607400	0.24817100	-1.53207900
	H	3.06186900	0.33428600	-2.39988900
	H	4.73769200	0.03127400	-1.89747200
	H	3.76545400	1.24616300	-1.06132800
	C	3.25630800	-0.79843300	-0.57045400
	C	1.78714300	-1.05392200	-0.38757200
	H	1.61872100	-2.12229700	-0.18389200

	H	1.24173800	-0.81549000	-1.30876900
	C	1.13087700	-0.30091700	0.79697300
	H	1.70021900	-0.50484400	1.71275500
	C	-0.33947400	-0.67567500	1.05527600
	H	-0.63845500	-0.27208100	2.02962800
	H	-0.38098700	-1.76787200	1.15547800
	C	-1.38467700	-0.24342800	0.01373600
	H	-1.14371500	-0.62644600	-0.98299100
	C	-2.80032900	-0.67886600	0.40853800
	H	-3.08358700	-0.14939400	1.32906500
	H	-2.77071000	-1.74698400	0.66391400
	C	-3.85274600	-0.43319600	-0.67964000
	H	-3.57907200	-1.00053000	-1.57981100
	H	-3.83237800	0.62491100	-0.96246400
	C	-5.26590000	-0.82714800	-0.23565100
	H	-5.58113800	-0.24853500	0.64070300
	H	-5.99572900	-0.64659500	-1.03183700
	H	-5.32102300	-1.88957600	0.03123700
	C	4.21509000	-1.31446000	0.45881400
	H	3.86287500	-2.24592000	0.91879500
	H	5.20437400	-1.50422100	0.02395400
	H	4.37392300	-0.59199100	1.27976100
	O	1.30934900	1.09865800	0.48595200
	O	-1.41758500	1.20765100	-0.10184000
	O	-0.70957300	1.62393800	-1.29953100
	H	0.21135900	1.64960100	-0.95856600
	O	0.79840700	1.90576800	1.58092800
	H	-0.13041900	2.02567500	1.29001100
CP1	C	4.59407300	-1.15635100	-0.55948700
	H	4.50147400	-1.25564100	-1.64705700
	H	4.56656100	-2.16544400	-0.12732300
	H	5.58135900	-0.73224800	-0.34569100
	C	3.47724400	-0.27424700	0.02027500
	H	3.54160500	0.71359600	-0.45256300
	C	2.09909800	-0.86301800	-0.33962300
	H	1.95876300	-1.81597200	0.19147000
	H	2.07774300	-1.09885700	-1.41259700
	C	3.66153400	-0.09315200	1.53543300
	H	2.92608800	0.59594500	1.96234500
	H	3.57426400	-1.05396800	2.06045500
	H	4.65359500	0.31525800	1.75749200
	C	0.90101300	0.04759900	-0.03528900
	H	0.92969800	0.38792000	1.00450100
	C	-0.42738700	-0.67500200	-0.32134600
	H	-0.44924400	-1.63888600	0.20467800
	H	-0.46964700	-0.92484100	-1.39226000
	C	-1.71722100	0.06695000	-0.00225400
	C	-2.97655700	-0.78262900	0.04854800
	H	-2.88372600	-1.43383700	0.93229200
	H	-2.96278400	-1.46952200	-0.81015200
	C	-4.28650300	0.00680400	0.10172900
	H	-4.34853600	0.65736600	-0.77853400
	H	-4.26633600	0.67617700	0.96817700
	C	-5.51604300	-0.90581300	0.16613000
	H	-5.49471100	-1.54429900	1.05749400
	H	-6.43908900	-0.31826900	0.20227400

	H	-5.57510900	-1.56210500	-0.71036600
	O	1.03415800	1.20976100	-0.87315500
	O	0.72488300	2.40611700	-0.11296100
	H	-0.25057600	2.31583000	-0.03020400
	O	-1.76240400	1.27474100	0.19622500
CT2	C	-4.45880300	-0.31178100	0.56829500
	H	-4.39513400	0.64336300	1.09919600
	H	-4.79723000	-1.06997900	1.29266300
	H	-5.23334900	-0.23001300	-0.20122900
	C	-3.12210700	-0.70877500	-0.02718000
	H	-2.76596300	0.28935300	-0.84511500
	C	-1.92516200	-0.63475800	0.91742100
	H	-1.62274600	-1.64646000	1.22719500
	H	-2.18932000	-0.07623300	1.82272900
	C	-0.69360100	0.05386200	0.27904800
	H	-0.31931100	-0.53354200	-0.56714600
	C	0.41260500	0.37240500	1.28810500
	H	0.45431700	-0.42664500	2.03787100
	H	0.12200500	1.28261100	1.82468000
	C	1.82529400	0.54504000	0.68911900
	H	2.44932100	1.07641800	1.42195500
	C	2.50237900	-0.78190100	0.32024100
	H	1.91323300	-1.28911800	-0.45587000
	H	2.46890700	-1.42523400	1.21024300
	C	3.95660100	-0.63742800	-0.14993300
	H	4.53183800	-0.11129600	0.62407700
	H	3.98655900	-0.00177300	-1.04084100
	C	4.61586200	-1.98812900	-0.44979900
	H	4.07946600	-2.52473400	-1.24160500
	H	5.65123400	-1.85807900	-0.78207600
	H	4.63033600	-2.63362900	0.43709400
	C	-3.15517900	-1.92017800	-0.94197300
	H	-2.18829700	-2.09222200	-1.42579900
	H	-3.40505900	-2.82479400	-0.36620500
	H	-3.91172000	-1.81169500	-1.72598200
	O	-1.14629000	1.32225900	-0.24325900
	O	-1.98701900	1.06799900	-1.35611900
	O	1.81494100	1.30282900	-0.52562000
	O	1.36505400	2.65201100	-0.22961300
	H	0.42008800	2.57278500	-0.46901200
CT1	C	-4.67749200	-1.34074800	-0.46999000
	H	-4.35959400	-2.38650500	-0.54980600
	H	-4.92005800	-0.98598100	-1.48023900
	H	-5.59802300	-1.31332100	0.12318900
	C	-3.58020700	-0.47272500	0.16648300
	H	-3.35550300	-0.88225000	1.15972900
	C	-2.29173300	-0.56184200	-0.67772900
	H	-2.46514500	-0.08792600	-1.65455200
	H	-2.06286400	-1.61685600	-0.87975300
	C	-1.04818200	0.08028700	-0.06662100
	H	-1.23148500	1.11709500	0.23159900
	C	0.17578800	0.02758700	-1.01619200
	H	0.03263100	0.75529600	-1.82312500
	H	0.21875500	-0.97421800	-1.45739000
	C	1.50479700	0.30287600	-0.31745100
	H	1.10436300	0.13724500	0.95433100

C	2.65604200	-0.65382400	-0.58202600
H	2.93609600	-0.57876400	-1.64545100
H	2.26387500	-1.66731700	-0.43373500
C	3.89876800	-0.44781300	0.29794800
H	3.60116900	-0.50330400	1.35297400
H	4.29844300	0.55938200	0.13785900
C	4.98761300	-1.48835500	0.01422100
H	5.32395200	-1.43903900	-1.02823900
H	5.86230900	-1.32701000	0.65267000
H	4.62413600	-2.50618900	0.19903400
C	-4.06725700	0.97399500	0.34425900
H	-3.32980300	1.59963900	0.85725300
H	-4.28548300	1.43699000	-0.62711600
H	-4.98725700	1.00211200	0.93844700
O	-0.72912700	-0.67370800	1.11623700
O	0.27383300	0.03175900	1.83245300
O	2.00705200	1.60778400	-0.43062300
O	0.94067900	2.57796100	-0.25264300
H	1.04116700	2.79391300	0.69153300

Table S6: Frequencies for α,γ -OOQOOH radical A, B, and C in Fig. 5 and derived transition states and products at the B3LYP/6-31+G(d,p) level of theory (cm^{-1}).

A	24.3616	40.8751	46.9018
	54.0297	87.7160	97.9585
	108.1411	123.0471	146.5021
	152.2271	157.2658	172.0156
	212.3146	244.6191	247.2637
	273.2476	312.6941	385.4827
	402.9628	429.1319	455.2391
	500.9061	533.2229	556.7340
	582.6810	729.7967	735.1282
	755.4198	796.2095	805.2641
	865.0563	882.6747	897.8623
	918.3163	934.3868	987.8624
	1003.9643	1027.0632	1029.3911
	1045.1870	1065.5074	1067.4423
	1068.9583	1082.6330	1121.4771
	1140.1302	1166.9318	1208.0171
	1216.2674	1231.0151	1252.7273
	1265.2312	1275.1193	1297.5275
	1312.4731	1327.0947	1328.0601
	1337.7863	1340.3948	1347.2000
	1372.9185	1383.3458	1390.4278
	1401.2608	1408.0495	1413.7417
	1418.8951	1434.9633	1475.4806
	1478.9082	1484.9210	1489.9815
	1491.2134	1495.5884	1502.5393
	1504.6264	1511.0441	1517.1688
	3003.3646	3005.6269	3011.6645
	3019.0783	3021.2128	3026.4336
	3028.0495	3030.0361	3034.6912
	3036.9014	3049.0032	3056.9851
	3060.9710	3064.7291	3080.4647
	3086.1493	3088.7573	3096.3250
	3101.6214	3117.9702	3620.8393
AP1	25.9264	39.7360	45.1643
	68.5906	86.1367	98.2515
	107.5842	133.2231	149.4507
	156.0572	176.7600	213.0062
	217.5718	246.5818	278.1957
	292.0579	377.0978	413.0934
	483.7786	522.8282	538.5905
	561.6045	595.0132	732.4045
	740.0461	770.9398	806.7589
	833.4532	885.2922	897.9498
	910.4251	951.7183	972.0437
	987.0751	994.9797	1025.4766
	1030.6673	1039.0751	1062.9166
	1066.9149	1079.2190	1103.4770
	1141.7026	1163.2753	1213.1212
	1228.1610	1243.4738	1269.4664
	1274.9510	1305.3397	1311.3293
	1324.5902	1332.8854	1335.2361
	1338.2386	1357.9437	1376.5542
	1392.3585	1405.6561	1406.7090

	1419.1263	1420.2637	1425.9292
	1476.5182	1485.8186	1490.0434
	1491.3734	1495.9100	1503.1156
	1504.6609	1511.3966	1517.1651
	1786.0110	2938.8653	3001.9779
	3004.2525	3008.8518	3013.4367
	3019.7886	3025.7751	3026.4291
	3029.5765	3033.7283	3035.7201
	3048.5406	3062.9178	3063.2973
	3074.2854	3090.1199	3095.6552
	3100.4193	3120.9082	3633.0938
AP2	17.4684	26.4537	31.6674
	54.2955	75.4217	99.4225
	106.2837	110.8510	129.6049
	147.4923	154.6378	184.2501
	207.2999	235.5102	245.1677
	246.8422	271.4703	279.0911
	339.1590	359.1425	416.2276
	443.5702	445.5880	484.2182
	521.2734	585.4489	613.2415
	731.0884	751.6060	793.7871
	817.1134	846.0440	897.2066
	902.7384	941.5151	951.8470
	964.6008	985.5822	994.8130
	1026.5210	1038.3396	1056.5992
	1066.5147	1067.6054	1083.2321
	1108.1232	1113.8025	1139.6173
	1151.9025	1204.9548	1223.5044
	1232.3640	1254.1264	1273.3633
	1284.2321	1290.0211	1314.2593
	1326.2267	1331.0759	1350.6320
	1357.9919	1366.3581	1385.6220
	1400.1168	1405.8337	1408.4880
	1417.5477	1428.8390	1439.6900
	1453.8670	1464.5208	1473.5468
	1491.2158	1494.5941	1504.4354
	1505.0742	1514.9168	1521.6945
	2913.8590	2932.1120	2989.5567
	3003.3258	3015.6103	3019.8919
	3022.7307	3027.9344	3029.3143
	3034.5907	3041.5261	3046.4375
	3049.5538	3066.4105	3081.2651
	3092.3370	3095.5273	3100.3535
	3181.8018	3612.2113	3767.7133
AT1	-1657.0382	25.5449	40.2319
	46.7158	65.4665	74.9717
	96.7651	104.0446	130.5957
	153.8498	159.2460	176.4740
	200.9795	225.3494	237.1130
	248.0755	267.9082	319.2325
	370.6829	402.2098	435.9878
	465.8551	503.1251	556.1754
	569.6412	662.7506	732.5092
	736.9837	762.9523	816.6749
	830.9519	855.5052	896.3132
	898.7577	913.8762	953.9164

	983.0229	988.0741	1004.7761
	1023.5176	1034.3325	1046.5886
	1065.9823	1067.3246	1075.9565
	1088.9136	1110.5796	1141.3802
	1171.8563	1202.0710	1218.1004
	1235.2665	1245.8161	1267.2628
	1279.0639	1307.1379	1313.5022
	1324.5019	1336.7009	1337.5178
	1342.6940	1353.7207	1365.7160
	1371.6047	1375.9920	1396.3831
	1406.3512	1409.9364	1419.3684
	1455.5588	1480.3177	1490.1627
	1491.4427	1495.9713	1503.0419
	1504.6778	1511.4110	1517.4643
	1605.3294	3002.1448	3004.6159
	3010.7177	3018.7042	3020.4663
	3025.1527	3027.1013	3029.4527
	3033.5109	3047.0949	3048.2549
	3056.3774	3063.2646	3069.6126
	3085.5288	3095.5008	3100.4672
	3104.6832	3127.1305	3735.8191
AT2	-1635.3991	22.7881	37.6877
	48.6944	58.3084	83.0772
	113.9006	127.6332	129.8525
	158.5928	173.2674	188.6383
	226.8945	246.1286	273.2481
	298.1529	311.4814	397.0505
	405.8422	432.5709	485.8788
	488.7115	509.8996	530.4300
	556.7674	621.9890	731.4990
	748.6537	799.2390	807.8095
	834.1694	873.9133	894.0798
	909.4789	916.2317	946.0309
	988.8181	991.7199	999.0269
	1015.8219	1042.7816	1046.8762
	1064.1142	1070.7945	1086.4565
	1101.5234	1121.0638	1143.3345
	1162.9772	1169.6931	1213.3357
	1234.3335	1243.2914	1262.6738
	1267.6033	1291.4738	1297.1283
	1322.3538	1332.0825	1334.1442
	1344.1102	1361.3751	1379.4114
	1394.7559	1404.5308	1406.5365
	1409.5192	1413.1840	1418.6963
	1468.1670	1472.0922	1475.4457
	1482.4423	1491.2254	1494.5430
	1504.5901	1505.2718	1515.0849
	1564.9663	2959.2401	3005.7960
	3009.4230	3014.3625	3021.3170
	3029.8809	3030.5877	3031.5501
	3034.7154	3049.2404	3051.8365
	3052.4482	3068.0171	3072.3059
	3079.4318	3088.2943	3097.0808
	3099.8416	3102.6564	3662.5789
B	30.9917	44.7715	51.9830
	65.5281	90.6140	102.6464

	117.8723	130.5133	154.1305
	167.9528	178.1080	211.8365
	224.5581	225.7768	248.7631
	277.7388	317.0659	326.8238
	357.0289	429.5074	450.5800
	479.3404	493.7640	535.5053
	570.8748	626.1550	729.7941
	738.4206	774.8888	825.2346
	835.8163	862.6410	898.6094
	907.3357	918.5310	959.2876
	968.9740	1000.4361	1012.6316
	1032.6428	1051.2793	1063.1943
	1068.7518	1087.3748	1121.4304
	1141.2712	1167.2772	1182.4556
	1209.3277	1219.1925	1236.0385
	1260.6112	1283.4636	1295.8293
	1320.0792	1324.2992	1334.1595
	1341.6889	1346.2510	1364.4146
	1366.4488	1387.9343	1397.3910
	1408.4695	1412.2717	1418.7963
	1419.7003	1436.1314	1477.5532
	1487.3462	1491.6463	1492.0489
	1493.1677	1499.7981	1504.8284
	1508.9620	1509.8874	1516.6050
	3005.0767	3008.6990	3018.4403
	3020.8696	3028.9135	3031.0276
	3031.7629	3037.8023	3041.6148
	3050.7874	3057.8203	3061.3201
	3064.4553	3081.7002	3089.2382
	3097.7365	3102.2561	3117.0706
	3121.8667	3134.6375	3615.0640
BP1	31.1597	40.0056	41.2408
	57.0455	78.6674	98.5346
	109.6538	122.3067	136.8137
	160.8094	178.6540	218.1781
	223.4023	251.0016	297.6838
	307.1399	350.5084	408.1175
	439.5138	464.7158	530.0776
	548.6896	613.2316	649.0627
	732.6544	742.4270	787.0651
	803.3773	836.9638	866.7260
	899.3018	932.2765	953.1893
	978.4335	988.9760	1008.1381
	1022.9552	1036.5169	1057.4223
	1068.5293	1076.7008	1089.5547
	1141.7275	1160.2840	1189.7672
	1217.7255	1238.3735	1255.6846
	1282.8604	1295.9353	1321.7481
	1329.6299	1336.0140	1338.2523
	1363.6547	1376.0232	1389.8976
	1401.2318	1405.8581	1409.7876
	1419.1907	1435.9070	1466.4815
	1470.3149	1480.3828	1482.6313
	1490.9630	1491.1493	1499.8986
	1505.2010	1509.3975	1516.4767
	1770.7280	3001.7062	3007.7079

	3015.3414	3017.5096	3020.0138
	3022.9483	3029.0273	3030.2820
	3039.9822	3042.3275	3052.0435
	3056.2369	3060.9129	3074.4871
	3089.9825	3096.8108	3100.3575
	3105.5016	3161.5896	3557.2925
BP2	23.5839	31.8525	43.5409
	59.2539	86.1933	118.1129
	122.1477	137.7997	143.6445
	173.8058	186.5775	206.8146
	238.3438	241.5814	258.0938
	301.4342	310.7861	334.6349
	356.1402	402.6854	438.6245
	444.2882	477.8866	494.8041
	534.3736	558.7360	646.1947
	696.9512	731.8910	778.7634
	800.1388	817.1777	861.1776
	894.8376	903.5997	924.4847
	946.4865	952.1569	979.1892
	992.9727	1016.4808	1032.5863
	1055.9183	1063.5820	1080.8483
	1102.5893	1123.5634	1140.2746
	1149.1152	1179.3641	1211.8304
	1231.5558	1238.5551	1265.0614
	1286.0409	1305.9707	1323.0791
	1328.6392	1349.8063	1363.8839
	1366.6312	1377.1708	1401.7410
	1407.8595	1417.8322	1421.5987
	1427.2970	1433.5472	1454.7641
	1457.0311	1472.4538	1479.8725
	1493.3090	1493.9063	1500.9062
	1503.8970	1509.5335	1513.9115
	2914.6483	2929.9983	2991.6344
	3012.5088	3017.7155	3020.2856
	3030.6212	3037.9619	3039.1954
	3050.0458	3054.8127	3063.1224
	3080.7605	3096.7442	3096.9966
	3101.3138	3127.8013	3134.3796
	3178.5912	3555.9086	3615.2076
BT1	-1624.8399	27.0607	34.0807
	44.7901	63.5315	72.9618
	106.4186	124.3102	141.5281
	153.3641	173.2809	187.3959
	206.0244	213.5418	246.0464
	249.6586	278.5193	284.2993
	339.6716	360.7910	420.2709
	435.3356	458.0859	504.6042
	528.3454	562.6389	635.4651
	731.1578	740.9393	784.8742
	847.2230	858.1271	880.6691
	898.0647	914.7969	947.2981
	968.2764	973.9179	993.1003
	1004.5053	1018.4003	1043.3142
	1050.3918	1063.4100	1068.2045
	1104.4394	1119.3831	1148.8959
	1178.5013	1200.7332	1226.0394

	1234.4693	1249.6922	1268.8020
	1281.2474	1294.9833	1320.3769
	1327.6709	1330.1406	1336.5037
	1357.9318	1368.1135	1370.2511
	1385.0823	1404.9951	1408.0828
	1409.8083	1418.4459	1455.7810
	1479.8691	1483.2542	1490.7807
	1490.8705	1492.1018	1499.6871
	1504.8243	1509.2764	1516.4578
	1598.8519	3002.9770	3007.2356
	3017.9646	3019.8019	3025.1034
	3027.0481	3029.0146	3030.1665
	3040.2649	3047.1081	3055.5661
	3060.3779	3069.2428	3085.7187
	3096.5058	3100.7859	3104.5129
	3107.2918	3140.6035	3733.2099
BT2	-1632.9562	22.9802	30.4320
	44.7106	62.3690	81.6512
	89.4141	112.7923	143.2135
	146.9764	186.7162	212.8332
	228.1253	243.1282	248.2451
	263.8098	283.6018	317.7934
	331.5984	369.1624	442.2202
	458.8159	480.7999	489.0235
	518.3250	552.3452	618.1750
	732.2654	770.8261	790.1787
	818.0123	864.9130	886.2317
	900.2190	925.2194	939.7300
	952.2805	973.6284	1002.5935
	1007.5983	1023.2981	1039.6089
	1050.6677	1066.3837	1101.3807
	1113.4991	1129.3464	1135.8178
	1150.8930	1165.5442	1169.1894
	1214.6845	1238.7579	1251.7721
	1270.5336	1285.4284	1310.2824
	1318.7483	1331.7876	1347.8029
	1353.6209	1364.0386	1370.0583
	1383.6956	1396.7164	1407.2472
	1412.2421	1416.8982	1421.4933
	1461.5386	1471.2811	1474.6950
	1490.7558	1493.0599	1501.0783
	1505.1733	1508.2386	1513.9278
	1574.2016	2957.1240	3009.2756
	3011.8961	3018.3783	3031.7604
	3032.9778	3040.4975	3042.6138
	3047.4021	3055.5505	3060.0838
	3063.9549	3073.5626	3088.0377
	3095.4694	3098.4290	3103.6129
	3113.9471	3140.1857	3756.9265
C	37.2002	38.7074	49.8890
	74.0645	79.1164	100.1786
	111.2094	142.5215	157.9738
	193.8972	201.3733	237.0029
	244.8514	248.1519	257.1225
	305.7324	327.6048	339.1488
	349.7224	374.3236	424.2809

	438.4906	461.9449	529.2103
	542.5613	573.1540	652.0238
	743.3690	771.7671	824.6599
	829.0012	847.9564	906.2807
	907.1467	935.2048	939.8863
	948.7457	967.1285	967.9737
	1005.6925	1015.4366	1052.5531
	1068.0607	1081.3856	1129.5046
	1151.9305	1163.6449	1180.8281
	1193.4114	1209.9792	1227.1361
	1257.4150	1279.8489	1287.0820
	1308.9696	1325.4971	1331.1200
	1351.9277	1364.3975	1371.0466
	1379.4904	1391.2326	1405.7657
	1409.3755	1412.0177	1420.1307
	1430.2542	1438.8710	1473.4872
	1481.6909	1486.9122	1493.2094
	1499.4462	1502.0319	1505.4318
	1510.7049	1513.5319	1517.3310
	3020.1409	3023.7948	3026.3148
	3027.2610	3029.3013	3029.6023
	3032.8635	3038.6017	3057.4849
	3063.4899	3066.3339	3081.5506
	3091.8866	3098.5715	3102.9530
	3103.5247	3106.0247	3106.5698
	3111.6513	3114.7029	3609.3089
CP2	37.9605	42.3548	54.0530
	73.5013	80.2877	98.2994
	118.5118	134.1077	138.1716
	146.2582	165.0039	192.9922
	242.9857	255.9796	270.3203
	298.2268	308.4572	331.9598
	354.6559	363.3380	391.6035
	424.7772	462.4742	517.9413
	535.5047	554.5302	659.2176
	694.5140	740.7337	781.1392
	802.5494	818.3809	854.9725
	897.0646	921.2201	928.9496
	941.0570	945.4671	959.5605
	987.3408	1006.3202	1009.9161
	1035.0753	1045.2429	1058.1293
	1075.5634	1086.9095	1128.5547
	1155.4232	1212.4060	1239.6014
	1267.1013	1278.4612	1282.8020
	1312.0011	1324.7369	1328.7030
	1339.3272	1357.7382	1369.4320
	1380.8515	1404.0408	1405.1416
	1410.9728	1420.1807	1420.5471
	1428.3902	1454.2311	1472.6917
	1473.6725	1474.2581	1482.9224
	1485.7718	1488.8777	1500.4408
	1501.0880	1505.0486	1513.7710
	2952.9645	2964.6114	3002.9468
	3019.8822	3028.7916	3030.7013
	3039.4271	3040.1738	3044.4727
	3049.8751	3056.5625	3070.2064

	3077.7592	3079.9943	3085.8923
	3091.3791	3092.8314	3102.2546
	3105.0754	3558.7354	3606.6355
CP1	27.6965	39.6985	42.8410
	67.8282	70.6015	105.6281
	116.7375	142.8242	188.5586
	221.5033	228.7314	241.0266
	242.8921	254.3937	302.7848
	338.7891	352.8334	372.7533
	402.8175	423.7140	462.3143
	528.0735	556.3563	640.6615
	695.9308	732.8417	801.4036
	802.0462	838.2634	879.0586
	884.2905	915.7319	934.2844
	954.1993	966.4590	968.1667
	998.8855	1027.2894	1040.3952
	1052.6364	1083.3901	1101.6342
	1143.6972	1154.7486	1166.3868
	1191.5647	1218.1413	1257.0260
	1279.9145	1286.5867	1317.1499
	1328.9577	1342.7285	1359.4420
	1378.7520	1387.3107	1397.8197
	1406.8360	1408.9863	1422.4135
	1428.1518	1436.9747	1455.8832
	1474.3421	1474.7144	1493.5432
	1496.2427	1501.6408	1505.9364
	1510.5058	1511.5256	1517.3477
	1765.0412	3006.8502	3011.0521
	3021.8041	3023.0962	3026.6392
	3031.0990	3041.9562	3046.0852
	3054.3612	3056.7545	3062.9395
	3082.5581	3085.0656	3087.7093
	3095.4381	3101.7639	3105.8152
	3108.4400	3111.2756	3547.1762
CT2	-1619.0202	35.6687	42.8492
	65.0710	81.9611	92.3272
	112.4627	139.2803	169.8498
	190.6340	196.5151	210.1766
	234.7014	245.8834	255.2809
	263.3440	304.9883	338.6435
	361.2430	383.7811	391.8686
	453.3657	484.9105	505.0459
	541.3954	547.9648	590.8448
	680.9393	742.4591	813.8903
	823.7502	836.4213	864.8597
	910.4070	912.4687	938.3474
	946.0910	973.3273	978.5131
	990.4876	992.1504	1010.4378
	1022.0290	1052.7657	1072.1676
	1087.4986	1114.1144	1142.8900
	1162.8601	1171.1600	1193.9486
	1244.7443	1249.6640	1266.3676
	1274.1225	1289.4306	1302.9807
	1329.7877	1341.3590	1364.8791
	1368.5288	1375.7060	1401.7008
	1404.5214	1411.1215	1419.5093

	1420.2258	1421.4873	1469.5037
	1478.8736	1481.0488	1482.6321
	1485.3021	1495.3250	1499.3544
	1504.1999	1505.3859	1513.2031
	1568.7083	2994.2635	3002.4231
	3011.0614	3017.9259	3021.3360
	3028.4511	3031.3219	3052.8747
	3059.8302	3066.7263	3078.0007
	3080.8894	3082.2886	3084.1291
	3095.0988	3102.4709	3105.1356
	3116.4474	3118.8886	3651.0165
CT1	-1614.3357	22.4176	36.6938
	54.9531	72.0472	84.5161
	88.3428	121.3339	132.0217
	190.0875	206.7175	221.6127
	233.9697	244.5024	250.9742
	255.4154	286.7734	302.2953
	329.0443	347.4989	389.1722
	418.9111	438.5026	455.9079
	498.6769	558.5994	588.0907
	649.0030	743.7548	805.2268
	827.0008	847.2692	869.2179
	901.6233	918.3193	932.5013
	939.2230	966.1023	973.8370
	977.7975	990.0402	1013.6527
	1045.2422	1066.4326	1072.6891
	1109.4282	1121.2367	1161.1171
	1172.5249	1190.7021	1191.7352
	1199.7194	1243.9357	1272.6994
	1288.3637	1292.7751	1320.7837
	1335.4321	1338.8713	1360.0706
	1364.4134	1371.6287	1380.2901
	1397.9236	1404.7780	1408.6604
	1420.0708	1427.5895	1459.1330
	1472.0221	1475.9720	1493.5070
	1499.9044	1500.4780	1504.8171
	1509.6650	1512.9911	1516.4165
	1595.6903	2992.8946	3018.4655
	3023.4524	3028.2496	3031.6373
	3040.9972	3042.3118	3048.6164
	3061.4427	3065.0780	3082.3897
	3085.5355	3089.2987	3096.6826
	3103.4993	3103.7165	3106.9826
	3108.0618	3110.7614	3732.6083

Table S7: Thermodynamic properties, standard enthalpy (kcal/mol), standard entropy (cal/mol/K), and heat capacities (300 – 1000 K) (cal/mol/K), for Benson Group Additivity.

Groups	ΔH^0_{298}	ΔS^0_{298}	Cp300	Cp400	Cp500	Cp600	Cp800	Cp1000
c/c/h3	-10.01	30.29	6.22	7.74	9.24	10.62	12.84	14.59
c/c2/h2	-5	9.65	5.59	7.08	8.34	9.53	11.23	12.48
c/c2/h/o	-7.04	-12.57	4.61	6.69	8.13	8.93	9.44	9.66
c/c/h2/o	-8.02	9.15	4.55	6.6	8.3	9.53	10.91	11.95
o/c/o	-5.5	8.54	3.9	4.31	4.6	4.84	5.32	5.8
o/h/o	-16.3	27.83	5.21	5.72	6.17	6.66	7.15	7.61
o/c/oj	12.6	36	7.1	7.38	7.8	8.08	8.76	9.7
c/c/co/h2	-5.41	9.02	5.62	6.89	8.01	9.35	10.99	12.19
co/c/h	-29.34	34.45	6.72	7.71	8.77	9.9	11.45	12.63
cj/c2/h	40.95	12.7	4.4	5.21	6.3	6.8	7.73	8.36
c/c/cj/h2	-4.95	9.42	5.5	6.95	8.25	9.35	11.07	12.34
co/c2	-31.5	15.14	5.59	6.09	6.81	7.48	8.54	9.14
c/co/h3	-10.31	30.8	6.47	8.03	9.48	10.59	12.68	14.26
c/c3/h	-2.09	-11.48	4.93	6.8	8.03	8.73	9.72	10.27
cj/c3	38	-10.77	4.06	4.92	5.42	5.75	6.27	6.35
c/cj/h3	-10.08	30.41	6.19	7.74	9.24	10.62	12.84	14.59

Table S8: Composition of groups for α,γ -OOQOOH radical A, B, and C in Fig. 5, and derived transition states and products.

Compound	group	quantity	group	quantity
A	c/c/h3	1	c/c2/h2	7
	c/c2/h/o	1	c/c/h2/o	1
	o/c/o	1	o/h/o	1
	o/c/oj	1		1
AP1	c/c/h3	1	c/c2/h2	6
	c/c2/h/o	1	c/c/co/h2	1
	o/c/o	1	o/h/o	1
	co/c/h	1		
AP2	c/c/h3	1	c/c2/h2	4
	cj/c2/h	1	c/c/cj/h2	2
	c/c2/h/o	1	c/c/h2/o	1
	o/c/o	2	o/h/o	2
B	c/c/h3	2	c/c2/h2	6
	o/c/o	1	o/h/o	1
	c/c2/h/o	2	o/c/oj	1
BP1	c/c/h3	1	c/c2/h2	5
	o/c/o	1	o/h/o	1
	co/c2	1	c/co/h3	1
	c/c2/h/o	1	c/c/co/h2	1
BP2	c/c/h3	2	c/c2/h2	3
	cj/c2/h	1	c/c/cj/h2	2
	o/c/o	2	o/h/o	2
	c/c2/h/o	2		
C	c/c/h3	3	c/c2/h2	4
	o/c/o	1	o/h/o	1
	c/c3/h	1	c/c2/h/o	2
	o/c/oj	1		
CP2	c/c/h3	1	c/c2/h2	3
	c/cj/h3	2	c/c/cj/h2	1
	cj/h3	1	c/c2/h/o	2
	o/c/o	2	o/h/o	2
CP1	c/c/h3	3	c/c2/h2	2
	o/c/o	1	o/h/o	1
	co/c2	1	c/c/co/h2	2
	c/c3/h	1	c/c2/h/o	1

Table S9: Reaction pathways and energy barriers for α,γ -OOQOOH radical A, B, and C in Fig 5. All in kcal/mol.

	Reactants	Transition States	Products	Energy Barrier
ΔH°_{298}	-69.3	-49.9	-103.6 + 8.9	19.3
Reaction	A	\rightarrow	AT1	\rightarrow
			AP1 + OH	
ΔH°_{298}	-69.3	-51.5	-57.6	17.8
Reaction	A	\rightarrow	AT2	\rightarrow
			AP2	
ΔH°_{298}	-73.3	-56.1	-111.1 + 8.9	17.2
Reaction	B	\rightarrow	BT1	\rightarrow
			BP1 + OH	
ΔH°_{298}	-73.3	-55.1	-61.7	18.2
Reaction	B	\rightarrow	BT2	\rightarrow
			BP2	
ΔH°_{298}	-75.4	-61.1	-69.8	14.3
Reaction	C	\rightarrow	CT2	\rightarrow
			CP2	
ΔH°_{298}	-75.4	-58.1	-113.3 + 8.9	17.3
Reaction	C	\rightarrow	CT1	\rightarrow
			CP1 + OH	

Table S10: Cartesian coordinates for ax-hydroperoxy-cyclohexyl-ax-peroxy (ax-OOH-ax-OO) and its radicals and transition states at the CBS-QB3 level of theory. Naming of species in Fig. S16.

RC			
C	-0.00486	-0.00731	-0.00042
C	-0.01052	-0.00672	1.533125
C	1.387618	-0.00173	2.14473
C	2.321755	-1.04784	1.545984
C	2.330197	-1.01672	0.010016
C	0.909932	-1.09617	-0.57016
O	0.519411	1.213618	-0.54185
O	-0.30682	2.31625	-0.10657
O	2.063433	1.300586	1.910882
O	1.352426	2.330747	2.310489
H	-1.03053	-0.13451	-0.36515
H	-0.52394	-0.90872	1.883374
H	-0.57804	0.845231	1.906334
H	1.329061	-0.09264	3.232535
H	1.981289	-2.02745	1.901625
H	3.330013	-0.90133	1.943385
H	2.934124	-1.84592	-0.36893
H	2.80583	-0.09416	-0.33034
H	0.934729	-1.00489	-1.65887
H	0.459106	-2.06826	-0.33848
H	0.250475	2.697618	0.594821
P1			
C	-0.01113	-0.02128	0.010576
C	-0.00875	-0.0289	1.503956
C	1.292011	-0.00702	2.241559
C	2.279557	-1.02709	1.651688
C	2.376604	-0.91768	0.122554
C	1.002361	-1.03277	-0.55402
O	0.442642	1.242655	-0.54139
O	-0.38236	2.297286	0.05576
O	1.973605	1.262179	2.101618
O	1.097361	2.312592	2.576802
H	-1.01678	-0.21267	-0.37819
H	-0.9442	0.046034	2.042893
H	1.13057	-0.19113	3.308794
H	1.940397	-2.02844	1.940028
H	3.258568	-0.87124	2.113406
H	3.036311	-1.70201	-0.26089

H	2.828708	0.04079	-0.13996
H	1.085496	-0.88689	-1.63511
H	0.582587	-2.03241	-0.39597
H	-0.37459	2.929124	-0.67569
H	0.63276	2.544931	1.7522

P2

C	-0.00758	-0.00466	-0.00194
C	-0.01994	-0.00492	1.530921
C	1.380927	0.006394	2.152732
C	2.328157	-0.92149	1.470763
C	2.26167	-1.14951	-0.00442
C	0.817536	-1.17294	-0.54725
O	0.629725	1.151228	-0.56365
O	0.04729	2.352901	-0.00677
O	1.802407	1.411488	2.051186
O	2.990781	1.59898	2.849259
H	-1.03999	-0.05443	-0.36935
H	-0.53465	-0.91167	1.863692
H	-0.59131	0.845044	1.90643
H	1.325399	-0.20953	3.22311
H	3.177922	-1.29519	2.031102
H	2.803893	-0.34384	-0.52392
H	0.825126	-1.13574	-1.63931
H	0.32038	-2.10364	-0.25542
H	0.683889	2.528051	0.707833
H	3.678533	1.580896	2.168744
H	2.778685	-2.07736	-0.26826

P3

C	-0.00826	-0.00401	-0.00205
C	-0.02255	-0.0063	1.532241
C	1.370783	0.005782	2.166499
C	2.281941	-1.09108	1.586675
C	2.192025	-1.20902	0.101648
C	0.853841	-1.14907	-0.56
O	0.598049	1.165842	-0.5664
O	-0.00269	2.352942	0.00386
O	1.87656	1.333461	1.927284
O	3.073051	1.520311	2.722545
H	-1.03937	-0.08139	-0.36868
H	-0.5367	-0.91499	1.863537
H	-0.60318	0.84078	1.899422
H	1.288224	-0.11609	3.251473
H	1.970688	-2.03685	2.068315

H	3.307622	-0.91873	1.921458
H	3.069656	-1.46862	-0.47667
H	0.950834	-1.0271	-1.64153
H	0.290461	-2.08571	-0.40155
H	0.650519	2.546056	0.697437
H	3.737853	1.594627	2.023734

P4

C	-0.00442	0.002921	0.005206
C	-0.00565	-0.01016	1.547177
C	1.373757	0.004687	2.20986
C	2.316728	-1.03542	1.604287
C	2.405387	-0.95128	0.070193
C	1.072823	-0.83251	-0.59168
O	-0.03052	1.364484	-0.52794
O	1.306186	1.912965	-0.63525
O	1.848778	1.360622	2.048552
O	3.140749	1.4918	2.692041
H	-0.98724	-0.3416	-0.33556
H	-0.5001	-0.92996	1.877166
H	-0.60812	0.826993	1.909621
H	1.267384	-0.1709	3.287044
H	1.935841	-2.02035	1.89821
H	3.305587	-0.92764	2.053247
H	2.950897	-1.81877	-0.31491
H	3.005392	-0.06962	-0.20508
H	0.980359	-1.08784	-1.64166
H	1.537412	2.083425	0.295837
H	2.897526	2.03232	3.45697

P5

C	-0.00101	0.005751	-0.00032
C	-0.00294	0.007149	1.533703
C	1.37834	-0.00441	2.137645
C	2.492585	-0.18336	1.430592
C	2.493645	-0.406	-0.05894
C	1.121054	-0.86249	-0.5701
O	0.166726	1.38851	-0.3629
O	0.072951	1.485317	-1.81111
H	-0.97512	-0.32731	-0.37946
H	-0.57241	-0.86433	1.881427
H	-0.56036	0.884604	1.880074
H	1.438346	0.148816	3.211764
H	3.45516	-0.15563	1.934182
H	3.255113	-1.14624	-0.32676

H	2.783116	0.523567	-0.56413
H	1.082857	-0.83391	-1.66042
H	0.934291	-1.89774	-0.26178
H	-0.76684	1.95699	-1.89397

P6

C	-0.00316	0.001818	-0.00196
C	-0.00435	-0.00512	1.503786
C	1.116614	-0.00172	2.226033
C	2.49794	0.048554	1.630476
C	2.472884	0.451376	0.150588
C	1.371884	-0.30552	-0.59791
O	-0.45546	1.327157	-0.35812
O	-0.76638	1.318953	-1.78298
H	-0.74766	-0.70936	-0.38059
H	-0.97414	-0.00977	1.990884
H	1.046928	-0.04266	3.310383
H	2.97372	-0.93573	1.751062
H	3.116668	0.744447	2.208048
H	3.448121	0.271345	-0.31012
H	2.271133	1.524203	0.07171
H	1.35747	-0.04648	-1.65855
H	1.544151	-1.38682	-0.52978
H	-1.72369	1.447551	-1.74544

TS1

C	-0.00576	-0.00733	0.000443
C	-0.00949	-0.0108	1.515059
C	1.353313	0.002177	2.228827
C	2.410101	-0.89128	1.581901
C	2.409709	-0.80487	0.04984
C	1.008055	-1.04112	-0.53129
O	0.445311	1.227647	-0.57311
O	-0.49918	2.275299	-0.25155
O	1.777143	1.375896	2.132174
O	0.592163	2.109162	2.421376
H	1.208584	-0.24998	3.28566
H	-0.16151	1.25854	1.979068
H	-0.77169	-0.64771	1.961703
H	-1.01075	-0.21744	-0.37958
H	1.019969	-0.97011	-1.62205
H	0.647788	-2.04297	-0.27177
H	3.105495	-1.54474	-0.35631
H	2.766363	0.178228	-0.26331
H	2.203842	-1.92042	1.898943

H	3.389702	-0.62822	1.992795
H	-0.02739	2.719474	0.47427
TS2			
C	-0.01219	0.009882	-0.00748
C	-0.02054	0.010752	1.525738
C	1.37014	-0.01049	2.149414
C	2.406836	0.886551	1.451822
C	2.345461	0.952839	-0.0573
C	0.889464	1.117877	-0.56145
O	0.539852	-1.18345	-0.58374
O	0.004043	-2.35688	0.067789
O	1.915357	-1.34112	2.016534
O	3.293729	-1.16262	2.303129
H	1.331858	0.24006	3.215119
H	3.331944	-0.01879	1.841191
H	2.613416	1.827386	1.961742
H	2.967209	1.770753	-0.42798
H	2.731772	0.023796	-0.48348
H	0.878464	1.085884	-1.65387
H	0.478891	2.086906	-0.25854
H	-1.04209	0.134356	-0.36498
H	-0.53155	0.920668	1.857257
H	-0.60335	-0.83253	1.900602
H	0.734928	-2.54536	0.681177
TS3			
C	-0.00855	-0.00946	-0.00407
C	-0.01086	-0.00389	1.539794
C	1.341145	0.001516	2.273927
C	2.353208	-0.95532	1.605932
C	2.452589	-0.53784	0.163629
C	1.175737	-0.78691	-0.61172
O	0.117246	1.27669	-0.64873
O	-0.46562	2.338915	0.130537
O	1.992774	1.276502	2.357722
O	2.173112	1.794876	1.051817
H	-0.95968	-0.44655	-0.33037
H	-0.51843	-0.9249	1.847725
H	-0.62739	0.82386	1.89022
H	1.188664	-0.25054	3.326306
H	1.980566	-1.98621	1.694271
H	3.30901	-0.89331	2.128912
H	3.390264	-0.73752	-0.35189
H	2.472831	0.812734	0.409088

H	1.269802	-0.49792	-1.66066
H	0.945233	-1.86248	-0.59452
H	0.343609	2.648001	0.575864

TS4

C	-0.01344	0.001176	0.000941
C	-0.01294	0.020354	1.547109
C	1.401439	-0.00808	2.138239
C	2.231987	1.196559	1.676068
C	2.019979	1.518909	0.167195
C	1.343357	0.371832	-0.55386
O	-0.42053	-1.32543	-0.35632
O	-0.5824	-1.35564	-1.80266
O	2.019549	-1.28673	1.823185
O	2.822595	-1.20374	0.660329
H	-0.77177	0.694665	-0.39272
H	-0.52532	0.920117	1.902301
H	-0.58344	-0.83945	1.903523
H	1.342695	-0.03007	3.229574
H	3.283206	0.990558	1.878552
H	1.945393	2.056022	2.287958
H	2.976014	1.747824	-0.30759
H	1.401231	2.421881	0.059353
H	1.415415	0.354068	-1.63931
H	2.138491	-0.66224	-0.12344
H	0.05128	-2.05116	-2.02545

TS5

C	-0.00338	0.004681	-1.2E-05
C	-0.01109	0.007337	1.530626
C	1.363418	-0.00382	2.120584
C	2.517809	0.287072	1.38964
C	2.424483	0.779226	-0.06448
C	0.981536	1.048588	-0.53165
O	0.466383	-1.23416	-0.54284
O	-0.39418	-2.30677	-0.08664
O	1.644434	-2.24694	2.044366
O	2.774144	-2.26932	1.455616
H	-1.01545	0.193433	-0.37493
H	-0.52129	0.919897	1.872772
H	-0.60658	-0.82557	1.909098
H	1.429357	-0.07388	3.200611
H	2.906095	-0.95231	1.315771
H	3.354877	0.678525	1.968666
H	2.884659	0.045676	-0.73129

H	3.01118	1.696271	-0.16713
H	0.642934	2.026502	-0.17294
H	0.938369	1.072988	-1.62285
H	0.182883	-2.71623	0.579818
TS6			
C	0.001976	-0.00504	-0.0115
C	0.002042	-0.04229	1.522212
C	1.203653	0.007955	2.23328
C	2.542509	0.205866	1.594024
C	2.441847	0.66049	0.134679
C	1.399498	-0.17851	-0.61402
O	-0.43813	1.254809	-0.55106
O	-1.8001	1.486215	-0.09755
O	0.908293	2.103006	2.949017
O	-0.25283	2.30769	2.465413
H	-0.67443	-0.7796	-0.3879
H	-0.80265	-0.6183	1.976984
H	-0.4093	1.160419	1.892742
H	1.206893	-0.3158	3.268613
H	3.064151	-0.76306	1.645233
H	3.143426	0.897777	2.191295
H	3.418328	0.57774	-0.34958
H	2.152944	1.714403	0.094765
H	1.664861	-1.24048	-0.56139
H	1.357658	0.093509	-1.67124
H	-1.68505	2.334021	0.354617

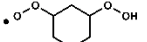
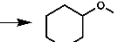
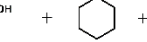
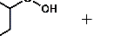
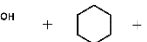
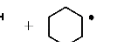
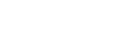
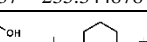
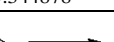
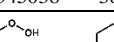
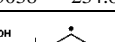
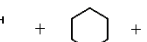
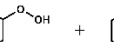
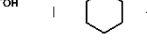
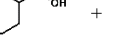
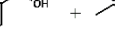
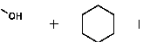
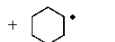
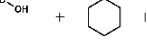
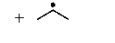
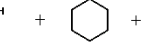
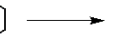
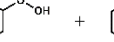
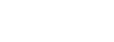
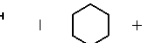
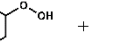
Table S11: Frequencies for ax-hydroperoxy-cyclohexyl-ax-peroxy (ax-OOH-ax-OO) and radicals and transition states at the B3LYP/6-311++G(2df,2pd) level of theory. Naming of species in Fig. S16.

Species' Names	Frequencies (cm ⁻¹)						
RC	87	100	133	181	223	254	322
	331	379	407	441	489	537	587
	710	775	804	827	875	883	916
	933	973	1020	1038	1078	1086	1140
	1144	1202	1227	1257	1292	1321	1341
	1352	1366	1380	1388	1402	1404	1413
	1473	1477	1489	1503	3020	3028	3031
	3048	3048	3065	3073	3080	3092	3115 3682
P1	88	113	142	178	187	216	245
	275	317	339	433	465	480	532
	587	626	737	800	806	862	882
	895	931	938	950	1007	1031	1057
	1117	1131	1167	1214	1286	1312	1327
	1340	1359	1366	1369	1385	1400	1415
	1442	1474	1484	1497	3025	3027	3037
	3040	3045	3068	3073	3094	3201	3673 3790
P2	81	88	113	157	198	247	272
	297	328	386	395	468	488	546
	572	606	731	779	804	852	874
	910	936	956	972	1009	1033	1083
	1086	1135	1170	1218	1265	1313	1329
	1340	1362	1368	1370	1388	1402	1411
	1413	1465	1474	1489	2956	3013	3040
	3048	3053	3060	3086	3102	3177	3693 3761
P3	80	86	119	151	189	250	258
	298	317	356	399	430	470	478
	598	602	768	816	825	852	876
	893	943	953	964	995	1065	1074
	1102	1123	1153	1238	1251	1277	1332
	1347	1353	1365	1378	1382	1404	1409
	1413	1461	1465	1480	2908	2927	3014
	3035	3050	3075	3077	3102	3189	3705 3771
P4	81	97	135	170	224	242	258
	281	351	376	413	458	478	538
	586	670	725	733	827	852	878
	895	931	944	958	1017	1046	1065
	1097	1139	1165	1206	1280	1311	1324
	1341	1364	1365	1376	1392	1400	1410

	1450	1464	1467	1491	2956	3015	3024	
	3032	3046	3050	3085	3095	3174	3655	3768
P5	88	127	185	213	283	348	391	
	436	569	603	658	765	816	861	
	889	910	941	975	1004	1009	1050	
	1084	1102	1170	1204	1244	1274	1334	
	1354	1365	1367	1388	1400	1428	1467	
	1478	1490	1716	3006	3017	3019	3032	
	3046	3049	3094	3139	3161	3778		
P6	83	140	200	228	268	327	430	
	464	516	581	712	736	827	853	
	890	908	935	960	1016	1022	1064	
	1088	1107	1165	1185	1260	1280	1339	
	1349	1365	1369	1376	1399	1428	1473	
	1488	1500	1704	2989	3008	3025	3033	
	3045	3075	3089	3141	3171	3778		
TS1	-2191	96	133	178	216	250	290	
	317	364	438	468	498	564	605	
	623	754	783	819	833	877	890	
	924	943	949	973	996	1042	1052	
	1091	1141	1151	1182	1222	1282	1306	
	1313	1351	1355	1376	1381	1391	1406	
	1422	1474	1484	1499	1704	3017	3029	
	3032	3042	3049	3067	3079	3097	3128	3685
TS2	-2160	58	127	148	223	244	286	
	330	380	432	451	504	544	596	
	675	719	798	820	826	877	889	
	926	937	964	983	994	1045	1082	
	1090	1128	1147	1191	1224	1264	1322	
	1330	1335	1357	1364	1377	1395	1403	
	1408	1470	1488	1493	1703	3008	3024	
	3040	3051	3052	3083	3091	3095	3117	3712
TS3	-1814	80	146	195	226	302	331	
	377	403	452	508	523	538	596	
	656	730	752	821	842	888	895	
	912	935	971	986	1019	1052	1057	
	1081	1116	1141	1151	1219	1252	1291	
	1313	1338	1345	1358	1378	1385	1403	
	1408	1463	1464	1479	1558	2984	2990	
	3010	3041	3073	3084	3095	3112	3126	3676
TS4	-1889	52	132	168	199	234	246	
	302	342	392	439	480	524	580	
	635	755	766	813	847	889	896	

	916	950	954	975	1026	1046	1095
	1105	1112	1153	1201	1242	1252	1275
	1322	1330	1337	1352	1367	1370	1380
	1391	1470	1475	1494	1513	2964	2982
	3047	3053	3068	3081	3098	3109	3131 3778
TS5	-908	84	115	135	169	205	230
	295	361	374	423	435	508	556
	591	692	761	798	819	850	899
	919	940	971	984	1023	1040	1083
	1118	1183	1184	1248	1262	1303	1320
	1335	1362	1368	1376	1393	1408	1417
	1456	1486	1501	1551	1567	2995	3027
	3040	3045	3071	3085	3089	3099	3181 3704
TS6	-1009	46	95	131	166	186	235
	267	288	364	383	455	486	550
	587	680	725	795	820	849	889
	935	938	969	981	1031	1054	1083
	1121	1161	1196	1242	1279	1296	1320
	1334	1359	1365	1376	1387	1391	1412
	1457	1484	1504	1548	1575	2975	3023
	3037	3045	3062	3082	3087	3114	3177 3770

Table S12: Isodesmic reactions and information for reference species. Naming of species present in Fig. S16.

RC					
 + ClI ₄ →  + CH ₃ OO [•]					
Exp. $\Delta_f H^\circ$ [kJ/mol] ^a	-74.87	-214.9	9.92		
Energy [Hartree]	-535.112013	-40.406188	-385.545038	-189.954761	
 +  +  →  +  + 					
Exp. $\Delta_f H^\circ$ [kJ/mol] ^a	-124.6	-124.6	-214.9	-214.9	75.839 ^b
Energy [Hartree]	-535.112013	-235.344878	-235.344878	-385.545038	-385.545038
P1					
 +  -  →  +  + 					
Exp. $\Delta_f H^\circ$ [kJ/mol] ^a	-124.6	-124.6	-214.9	-214.9	75.839 ^b
Energy [Hartree]	-535.087637	-235.344878	-235.344878	-385.545038	-385.545038
  -  →  -  + 					
Exp. $\Delta_f H^\circ$ [kJ/mol] ^a	-124.6	-104.7	-214.9	-214.9	90
Energy [Hartree]	-535.087637	-235.344878	-118.850369	-385.545038	-385.545038
P2					
 +  +  →  +  + 					
Exp. $\Delta_f H^\circ$ [kJ/mol] ^a	-124.6	-124.6	-214.9	-214.9	75.839 ^b
Energy [Hartree]	-535.088858	-235.344878	-235.344878	-385.545038	-385.545038
  +  →  +  + 					
Exp. $\Delta_f H^\circ$ [kJ/mol] ^a	-124.6	-104.7	-214.9	-214.9	90
Energy [Hartree]	-535.088858	-235.344878	-118.850369	-385.545038	-385.545038
P3					
 +  +  →  +  + 					
Exp. $\Delta_f H^\circ$ [kJ/mol] ^a	-124.6	-124.6	-214.9	-214.9	75.839 ^b
Energy [Hartree]	-535.088586	-235.344878	-235.344878	-385.545038	-385.545038
  +  →  +  + 					
Exp. $\Delta_f H^\circ$ [kJ/mol] ^a	-124.6	-104.7	-214.9	-214.9	90
Energy [Hartree]	-535.088586	-235.344878	-118.850369	-385.545038	-385.545038
P4					
 +  +  →  +  + 					
Exp. $\Delta_f H^\circ$ [kJ/mol] ^a	-124.6	-124.6	-214.9	-214.9	75.839 ^b
Energy [Hartree]	-535.084927	-235.344878	-235.344878	-385.545038	-385.545038
  +  →  +  + 					
Exp. $\Delta_f H^\circ$ [kJ/mol] ^a	124.6	-104.7	-214.9	-214.9	90
Energy [Hartree]	-535.084927	-235.344878	-118.850369	-385.545038	-385.545038
P5					

Exp. $\Delta_f H^\circ [kJ/mol]^a$	-124.6	-214.9	-4.32
Energy [Hartree]	-384.337369	-235.344878	-385.545038
Exp. $\Delta_f H^\circ [kJ/mol]^a$	-104.7	-214.9	20.41
Energy [Hartree]	-384.337369	-118.850369	-385.545038
P6			
Exp. $\Delta_f H^\circ [kJ/mol]^a$	-124.6	-214.9	-4.32
Energy [Hartree]	-384.337776	-235.344878	-385.545038
Exp. $\Delta_f H^\circ [kJ/mol]^a$	-104.7	-214.9	20.41
Energy [Hartree]	-384.337776	-118.850369	-385.545038

^a all Exp. $\Delta_f H^\circ$ from NIST Chemistry WebBook (except ^b from Ref. (19))

References

1. Hansen N, Cool TA, Westmoreland PR, & Kohse-Höinghaus K (2009) Recent contributions of flame-sampling molecular-beam mass spectrometry to a fundamental understanding of combustion chemistry. *Prog. Energy Combust. Sci.* 35(2):168-191.
2. Qi F (2013) Combustion chemistry probed by synchrotron VUV photoionization mass spectrometry. *Proc. Combust. Inst.* 34:33-63.
3. Wang Z, et al. (2018) n-Heptane cool flame chemistry: Unraveling intermediate species measured in a stirred reactor and motored engine. *Combust. Flame* 187(Supplement C):199-216.
4. Dagaut P, et al. (1986) A jet-stirred reactor for kinetic studies of homogeneous gas-phase reactions at pressures up to ten atmospheres (1 MPa). *J. Phys. E: Sci. Instrum.* 19:207–209.
5. Raffaelli A & Saba A (2003) Atmospheric pressure photoionization mass spectrometry. *Mass Spectrom. Rev.* 22(5):318-331.
6. Battin-Leclerc F, et al. (2010) Experimental confirmation of the low-temperature oxidation scheme of alkanes. *Angew. Chem. Int. Edit.* 49(18):3169-3172.
7. Dodson LG, et al. (2015) VUV photoionization cross sections of HO₂, H₂O₂, and H₂CO. *J. Phys. Chem. A* 119(8):1279-1291.
8. Wang Z, et al. (2016) Additional chain-branching pathways in the low-temperature oxidation of branched alkanes. *Combust. Flame* 164:386-396.
9. Wang Z, et al. (2017) New insights into the low-temperature oxidation of 2-methylhexane. *Proc. Combust. Inst.* 36:373–382.
10. Frisch MJ, et al. (2009) Gaussian 09, Revision D.01, Wallingford CT.
11. Benson SW (1976) *Thermochemical Kinetics* (Wiley-Interscience, New York).
12. Sheng C (2002) Elementary, Pressure Dependent Model for Combustion of C1, C2 and Nitrogen Containing Hydrocarbons: Operation of A Pilot Scale Incinerator and Model Comparison. (New Jersey Institute of Technology, New Jersey, U. S.).
13. Lay TH, Krasnoperov LN, Venanzi CA, Bozzelli JW, & Shokhirev NV (1996) Ab Initio Study of α -Chlorinated Ethyl Hydroperoxides CH₃CH₂OOH, CH₃CHClOOH, and CH₃CCl₂OOH: Conformational Analysis, Internal Rotation Barriers, Vibrational Frequencies, and Thermodynamic Properties. *J. Phys. Chem.* 100(20):8240-8249.
14. Fernandes RX, Zador J, Jusinski LE, Miller JA, & Taatjes CA (2009) Formally direct pathways and low-temperature chain branching in hydrocarbon autoignition: the cyclohexyl + O₂ reaction at high pressure. *Phys. Chem. Chem. Phys.* 11(9):1320-1327.
15. Montgomery Jr. JA, Frisch MJ, Ochterski JW, & Petersson GA (2000) A complete basis set model chemistry. VII. Use of the minimum population localization method. *J. Chem. Phys.* 112(15):6532-6542.
16. Yang Y, Boehman AL, & Simmie JM (2010) Uniqueness in the low temperature oxidation of cycloalkanes. *Combust. Flame* 157(12):2357-2368.
17. Zhang K, et al. (2016) An updated experimental and kinetic modeling study of *n*-heptane oxidation. *Combust. Flame* 172:116-135.
18. CHEMKIN-PRO 15112, Reaction Design: San Diego, (2012).
19. Goos E, Burcat A, & Ruscic B, Extended Third Millennium Ideal Gas and Condensed Phase Thermochemical Database for Combustion with updates from Active Thermochemical Tables.